



HAL
open science

The quadrupedal walking gait of the olive baboon, *Papio anubis*: an exploratory study integrating kinematics and EMG

François Druelle, Anthony Supiot, Silke Meulemans, Niels Schouteden, Pablo Molina-Vila, Brigitte Rimbaud, Peter Aerts, Gilles Berillon

► To cite this version:

François Druelle, Anthony Supiot, Silke Meulemans, Niels Schouteden, Pablo Molina-Vila, et al.. The quadrupedal walking gait of the olive baboon, *Papio anubis*: an exploratory study integrating kinematics and EMG. *Journal of Experimental Biology*, 2021, 224 (14), pp.jeb242587. 10.1242/jeb.242587. mnhn-03431584

HAL Id: mnhn-03431584

<https://mnhn.hal.science/mnhn-03431584>

Submitted on 17 Nov 2021

HAL is a multi-disciplinary open access archive for the deposit and dissemination of scientific research documents, whether they are published or not. The documents may come from teaching and research institutions in France or abroad, or from public or private research centers.

L'archive ouverte pluridisciplinaire **HAL**, est destinée au dépôt et à la diffusion de documents scientifiques de niveau recherche, publiés ou non, émanant des établissements d'enseignement et de recherche français ou étrangers, des laboratoires publics ou privés.

1 **The quadrupedal walking gait of olive baboon, *Papio anubis*: an exploratory**
2 **study integrating kinematics and EMG**

3 François Druelle^{a,b,c}, Anthony Supiot^d, Silke Meulemans^c, Niels Schouteden^{c,e}, Pablo Molina-Vila^b,
4 Brigitte Rimbaud^b, Peter Aerts^{c,f}, Gilles Berillon^{a,b}

5 ^aHistoire Naturelle de l'Homme Préhistorique, UMR 7194-MNHN-CNRS, Paris, France

6 ^bPrimate Station of the CNRS, UPS 846, Rousset-sur-Arc, France

7 ^cFunctional Morphology Laboratory, University of Antwerp, Wilrijk, Belgium

8 ^dGait and Motion Analysis Laboratory, Assistance Publique des Hôpitaux de Paris (AP-HP), Robert
9 Debré University Hospital, Paris, France

10 ^eMonde Sauvage Safari Parc, Aywaille, Belgium

11 ^fDepartment of Movement and Sports Sciences, University of Ghent, Gent, Belgium

12 **ABSTRACT** Primates exhibit unusual quadrupedal features (e.g. diagonal gaits, compliant walk)
13 compared to other quadrupedal mammals. Their origin and diversification in arboreal habitats have
14 certainly shaped the mechanics of their walking pattern to meet the functional requirements
15 **necessary for** balance control in unstable and discontinuous environments. In turn, the requirements
16 for mechanical stability **probably conflict** with the mechanical energy exchange. In order to
17 investigate these aspects, we have conducted **an integrative** study on quadrupedal walking in olive
18 baboon (*Papio anubis*) at the Primatology station of the CNRS in France. Based on kinematics, we
19 describe the centre of mass mechanics of the normal quadrupedal gait performed on the ground, as
20 well as in different gait and substrate contexts. In addition, we have studied the muscular activity of
21 six hind limb muscles using non-invasive surface probes. **Our results show that baboons can rely on**
22 **an inverted pendulum-like exchange of energy (57% in average and the maximal observed value is**
23 **84%)** when walking slowly ($<0.9\text{m}\cdot\text{s}^{-1}$) with a tight limb phase ($\approx 55\%$) on the ground using diagonal
24 sequence gaits. In this context the muscular activity is similar to **that of** other quadrupedal mammals
25 thus reflecting the primary functions of the muscles for limb movements and support. On the other
26 hand, walking on a suspended branch generates kinematic and muscular adjustments to ensure a
27 better control and to **maintain** stability. Finally, walking using the lateral sequence gait increases
28 muscular effort and reduces the potential for high recovery rates. **The present exploratory study thus**
29 **supports the assumption that primates are able to make use of an inverted-pendulum mechanism on**
30 **the ground using the diagonal walking gait**, yet a different footfall pattern and substrate appear to
31 influence muscular effort and efficiency.

32 **Key words** Centre of mass, Electromyography, kinematics, Locomotion, Positive reinforcement

33 INTRODUCTION

34 The origin and evolution of primates is closely related to arboreal habitats (e.g. Cartmill 1974;
35 Hamrick 2001; Toussaint et al. 2020) and many extant primates continue to live in arboreal
36 environments, or at least invest a certain amount of time foraging in the trees on thin and flexible
37 branches (Hunt 2016). Such an environment obviously implies discontinuity, variability, instability and
38 oscillations of the substrates that perturb the inherent mechanical requirements of legged
39 locomotion, i.e. propulsion, balance and stability of the walking gait. It has been shown that primates
40 exhibit a set of morphological adaptations and kinematical adjustments coupled to a behavioural
41 flexibility that allow them to meet the functional requirements demanded by this complex
42 environment (e.g. Cartmill et al. 2020; Demes et al. 1994; Druelle et al. 2020; Hunt et al. 1996; Larney
43 & Larson 2004; Larson et al. 2001; Schmitt 1999; Schmitt et al. 2006; Thorpe et al. 2007). During
44 quadrupedal walking, primates use diagonal sequence/diagonal couplet (DSDC) gaits, large limb
45 angular excursions, large elbow yield, long stance phase, low stride frequency, and a weight support
46 shifted toward the hind limbs (see Larson 2018 for a review). These features can be integrated under
47 the compliant gait model of primate walking (Schmitt 1999). Overall, these characteristics should
48 particularly allow for control pitching, yawing and rolling moments, and limit the vertical oscillations
49 of the centre of mass, hence branch oscillation, and increase maintenance of balance (e.g. Cartmill et
50 al. 2020; Cartmill et al. 2002; Schmitt et al. 2006).

51 Parallel to these functional adjustments, the muscular activity pattern also presents specificities. EMG
52 studies on non-human primates have provided a significant knowledge about muscle basic activity
53 pattern in different locomotor modes such as climbing, brachiating and bipedal walking (e.g. Hirasaki
54 et al. 1995; Ishida et al. 1974; Jungers & Stern 1981; Stern Jr & Larson 2001; Stern & Susman 1981),
55 but the way muscle recruitment has been altered in non-human primates in relation to the arboreal
56 niche remains poorly understood (Boyer et al. 2007; Courtine et al. 2005; Larson & Stern 2009; Patel
57 et al. 2015). During primate quadrupedal walking, distal limb muscles are suggested to be under
58 higher cortical control including different speed-related modulations of the limbs compared to other
59 quadrupedal mammals (Courtine et al. 2005). The different inertial properties of non-human
60 primates compared to other quadrupeds (Grand 1977; Druelle et al. 2019) should also affect the way
61 the work is performed, and the forces transmitted. Overall, more flexible capabilities of the
62 neuromotor control are suggested in primates (Courtine et al. 2005; Jungers & Anapol 1985; Shapiro
63 et al. 1997) with the hand and the foot having distinct functional roles (Druelle et al. 2018; Hashimoto
64 et al. 2011; Lawler 2006; Patel et al. 2015). Furthermore, although the phasic recruitment of muscles
65 is generally similar to other quadrupedal mammals (Courtine et al. 2005; Higurashi et al. 2019;
66 Shapiro & Jungers 1994), specificities have been emphasized for the humeral retractors (Larson &

67 Stern 1987; Larson & Stern 1989; Larson & Stern 2007), and hip extensors might also be used for
68 different functions (Larson & Stern 2009; Reynolds 1985). As a result, primate quadrupedal control
69 and mechanics are considered particular compared to that of other (terrestrial) quadrupedal
70 mammals. However, basic biomechanical and physiological data regarding the typical quadrupedal
71 walking pattern of non-human primates is, unfortunately, non-existent. Integrative studies examining
72 the kinematics, the dynamics of the centre of mass and the muscular activity (EMG) all together are
73 very rare (see Courtine et al. 2005).

74 To explore the quadrupedal walking gait of non-human primates and the suggested neuromotor
75 flexibility, we conducted an integrative analysis exploring the limb kinematics, the centre of mass
76 mechanics (using kinematics) and the muscle activity of six extrinsic hind limb muscles in olive
77 baboons, *Papio anubis*. Baboons can be considered as (semi-)terrestrial primates as they have
78 developed a set of cursorial adaptations that mean they are more suited for terrestrial locomotion
79 and for long-distance walking. For instance, they have been shown to move between 3.6 to 9.5 km
80 per day, making them the non-human primates with the longest daily travel distance (Garland 1983);
81 their limbs are relatively extended with a digitigrade hand posture when walking, they display
82 convergent natural pendular periods of their fore- and hindlimbs and their proximal limb mass
83 distribution suggests good propulsive action capacities (Druelle et al. 2017a; Patel 2009; Patel et al.
84 2012; Raichlen 2004; Zeininger et al. 2017).

85 In this study, animals were trained to voluntarily cooperate using positive reinforcement techniques.
86 Our refined experiment used surface probes (sEMG) that did not need surgical procedures. We first
87 recorded the muscular activity of two female baboons walking quadrupedally using their typical DSDC
88 gait over a flat regular ground at their voluntary walking speed. This allowed us to describe their
89 typical quadrupedal walking gait in terms of spatio-temporal parameters and muscular activity. We
90 then recorded the gait of one female baboon when walking DSDC on a suspended horizontal and
91 cylindrical substrate (branch) and while spontaneously using lateral sequence/lateral couplet (LSLC)
92 gaits for few strides on the ground. We thus provide a preliminary picture of the normal quadrupedal
93 walking pattern in baboon and its flexibility (through kinematic modulation) in the context of
94 different gait and substrate. First, and because the baboon is defined as an adapted quadrupedal
95 walker, we expect it to be able to make use of an inverted-pendulum mechanism when walking
96 steadily on the ground using its preferred walking gait (DSDC; as previously observed in ring-tailed
97 lemurs and capuchin monkeys: O'Neill & Schmitt 2012; Demes & O'Neill 2013). Second, we will
98 specifically evaluate whether the usual muscle activation pattern observed in DSDC walking is altered
99 in other gait and substrate contexts. When the baboon uses the unusual LSLC gait on the ground,
100 changes are expected in proximal muscles (i.e., in the main limb motors), while walking on a different

101 substrate, such as a branch (imposing higher balance requirements and certainly higher control),
102 should mainly affect the recruitment of distal muscles (Boyer et al. 2007; Courtine et al. 2005; Patel et
103 al. 2012). Exploring the kinematics, the movements of the centre of mass and the muscle activity
104 together should provide an integrative picture of the quadrupedal walking pattern in baboon and
105 how these are connected (see Courtine et al. 2005). In this context, a reduced efficiency in the
106 mechanics of the centre of mass (for example, walking on a branch requires kinematical adjustments
107 that tend to reduce the vertical oscillations of the centre of mass; see Gàlvez-López et al. 2011;
108 Schmitt 1999) should match an alteration of the muscular activity toward an increased activation.

109 MATERIALS AND METHODS

110 Context of experiment, training and study subjects

111 The olive baboons, *Papio anubis*, were housed at the Primatology Station of the CNRS (Rousset-sur-
112 Arc, France). The experiments presented in this study and conducted inside the primatology centre
113 are part of a large ongoing project on bipedal walking skills in non-human primates (Berillon et al. *in*
114 *preparation*). The heterogeneous character of the quadrupedal data presented here results from
115 opportunistic periods of data collection that were not initially intended **to be considered together**. All
116 the procedures that are described in this study were approved by the ethical committee on animal
117 experimentation n°14 (Projet 68-19112012, CEEA-14 Marseille).

118 Prior to the experiments, primates were trained over a period of **18 months** and focused on the
119 habituation and desensitization of individuals to the whole experimental setup. All the training was
120 based on positive reinforcement techniques and systematic desensitization (Prescott & Buchanan-
121 Smith 2016; Schapiro et al. 2003) and was conducted by the same two trainers, PMV and BR. The first
122 training period was carried out in a large indoor cage where the two individuals were pair-housed for
123 18 months. During this period, individuals were mainly habituated to the close proximity **of** and
124 interaction with trainers by means of training other basic behaviours as target or parking training.
125 After 6 months of training (46 sessions of training of **approximately** 30-45 minutes), individuals
126 **cooperated** to get out of their enclosure on a leash and to walk quadrupedally beside the trainer on
127 the experimental setup. Individuals were then moved to a bigger indoor/outdoor enclosure where
128 they could **move freely**. This training allowed us to lead the baboons to the technical platform for
129 data collection.

130 Training sessions started **when** the baboons were 1.5 and 2 years old. The collection of the data
131 presented in this study was performed during three recording sessions for individual 1 (Id1), the
132 04/07/2013, the 31/07/2013 and the 15/12/2017, and during one recording session for individual 2

133 (Id2), the 03/12/2013. At the time of data collection, Id1 was 3 years old and weighed 8.14 kgs in
134 2013 and 7.5 years old and weighed 13.5 kgs in 2017. Id2 was 3.5 years old and weighed 8.05 kgs in
135 2013. At 3 years of age, olive baboons have already experienced significant growth-related changes in
136 body morphometrics and their general morphotype is very similar to that of adults (see Fig. 6 in
137 Druelle et al. 2017). The maturation of their neuromotor control also appears to be largely complete
138 (see Druelle et al. 2017; Rose 1977), as has also been observed in other cercopithecoid species at this
139 age (e.g., Vilensky and Gankiewicz 1990; Zeininger et al. 2017; Dunbar and Badam 2000).

140 **Data collection**

141 *Surface electromyography (sEMG)*

142 Muscle activity was recorded at 2000Hz using a wireless Zerowire system (Aurion Srl, Milan, Italy)
143 with the MyoResearch XP Master Edition software (Noraxon®). We focused on 6 muscles commonly
144 studied as actuator of the three main joints of the hindlimb (hip, knee and ankle), and easily
145 identifiable at the surface of the skin: *gluteus medius*, *biceps femoris*, *rectus femoris*, *tibialis anterior*,
146 *gastrocnemius (medialis or lateralis)* and *peroneus longus*, of the right side (Figure 1). To ensure the
147 accurate electrode placement, the muscular topography was previously assessed on olive baboon
148 cadavers of a similar size and age that were available at the primatology station. Baboons were
149 instrumented during a short period of anaesthesia (≈60 minutes); the anaesthesia was initiated with
150 an intra-muscular injection of Ketamine (4mg/kg) and medetomidine (40µg/kg) and maintained with
151 gas isoflurane (1%). This anaesthesia was short and light enough to shorten the recovery period using
152 an atipamezole as antagonist. After locally shaving, cleaning and degreasing the skin, electrodes were
153 taped at the level of the muscles' belly (approximately at mid length of each muscle and electrode
154 pairs and always parallel to fibre direction). We used fabric legwear and trunkwear (close-fitting
155 clothes, see Fig. 6B) to ensure a good adhesion of the equipment and to protect the electrodes. In
156 the context of the present study, we have worked on the technical platform for biomechanics
157 (Motion analysis of Primates, MAP) that is permanently installed in an outdoor enclosure of the
158 primatology centre (see Berillon et al. 2011 for details). The experiments started after the baboons
159 were totally recovered from the anaesthesia (i.e. they were fully active and able to climb and run),
160 between 60 to 90 minutes after their arrival in the enclosure.

161 *Kinematics*

162 The animals walked on a straight and horizontal calibrated walkway and on a horizontal branch (∅
163 0.16 m, positioned at approximately 1m above the ground), where they could easily be video-
164 captured using an integrated multicamera system (Norpix Inc.) with 3 synchronized HD-video cameras

165 running at 200 frames per second (fps; Baumer HXC1) (see Berillon et al. 2010 for a general
 166 description of the experimental setup); synchronized recording was proceeded with Streampix 4 (by
 167 Norpix Inc.). Two cameras were laterally placed perpendicular to the walkway, to accurately record in
 168 a large field of view the main sagittal spatiotemporal and joints kinematics. **One additional** camera
 169 was positioned obliquely to increase the accuracy for visually identifying the locomotor events, i.e.
 170 touch-down and lift-off of the limbs. EMG and video recordings were synchronized using an external
 171 digital signal; in addition, a fourth lateral video camera (running at 60fps) was driven by the
 172 MyoResearch XP software and thus software-synchronized with the EMG recording.

173 We first qualitatively selected appropriate quadrupedal sequences during which the individual was
 174 walking steadily, along the platform or the branch. The quadrupedal strides were defined from a right
 175 hind limb touchdown to the next right hind limb touchdown. As we noticed some speed variation
 176 between consecutive quadrupedal strides, we calculated an acceleration/deceleration index as
 177 follows: $(average\ speed\ stride_{n+1} - average\ speed\ stride_n) / average\ speed\ stride_n$. For the present
 178 analysis, we removed the quadrupedal strides for which speed variations were above 10% between
 179 consecutive strides (note that given the small amount of lateral sequences recorded (n=6), we kept
 180 one stride for which the speed variation was 26% in order to keep a sample of 4 strides and,
 181 therefore, use non-parametric statistics, see further). Table 1 shows the dataset included in the
 182 present analysis after applying this strong selective criterion.

TABLE 1. Studied individuals and data collected

Individual	n/n ¹	EMG	Spatio-temporal	Kinematics (joint + BCoM)	Gait type / substrate
ID1					
04/07/2013	3/4	X	X	X	Diagonal / on ground
	2/3	X	X	X	Lateral ² / on ground
31/07/2013	9/14	X	X		Diagonal / on ground
15/12/2017	12/16	X	X	X	Diagonal / on ground
	2/3	X	X	X	Lateral / on ground
	6/8	X	X	X	Diagonal / on branch
ID2					
03/12/2013	19/39	X	X		Diagonal / on ground

¹the left side of the oblique sign indicates the number of strides kept in the present analysis and the right side indicates the total number of strides recorded before applying the acceleration selection criterion (see Methods)

²given the small amount of data for the lateral walking gait (2 in 2013 and 2 in 2017), we have pooled these data together in the analyses

183 Analysis

184 Basic kinematics

185 We calculated the following spatiotemporal parameters: the cycle duration (time period between two
 186 right hind limb touchdown events), the frequency (inverse of cycle duration), the duty factor

187 (proportion of stance phase of the right hind limb relative to cycle duration), stride length (horizontal
188 displacement of the tip of the right foot during one stride), speed (estimated from the horizontal
189 displacement of the centre of mass; see below) and limb phase (time period between the right hind
190 limb touchdown and the right forelimb touchdown relative to the cycle duration; <50% is a lateral
191 sequence, >50% is a diagonal sequence). The spatiotemporal parameters were made dimensionless
192 using geometric scaling equations (Hof 1996) and the shank length was used as the scaling factor
193 (Aerts et al. 2000). A total of 20 anatomical reference points were digitized by SM and NS using the
194 *DLTdv7* application developed in MATLAB by the T. Hendrick Lab (Figure 2). Video footage was
195 analysed for one individual and the kinematics were therefore extracted for Id1 in different contexts
196 (see Table 1). When the tracked anatomical references were obscured by the movement of other
197 limbs, we applied a piecewise linear interpolation to add the missing datapoints. Movement patterns
198 were visually checked using a custom-made script in MATLAB to ensure satisfactory digitization result,
199 i.e. a smooth movement with no anomaly. Data were then filtered per stride using a 4th order zero
200 phase shift Butterworth low pass filter with a cut-off frequency of 5Hz. We then applied a cubic spline
201 interpolation over a time base with 100 points in order to stride-normalized the individual
202 quadrupedal cycles. Tracking the joints and body segments during the walking strides allowed us to
203 measure 6 internal joint angles (joint extension accords to their increase) (Anvari et al. 2014): the
204 ankle [estimated between the foot taken as a whole (from heel to tip) and the shank segment], the
205 knee, the hip, the shoulder, the elbow and the wrist, as well as 5 external joint angles (with respect to
206 the horizontal): the shank, the thigh, the trunk, the humerus and the forearm.

207 *Centre of mass Mechanics*

208 The position of the body centre of mass (BCoM) can be estimated using body segment displacements
209 and morphometrics (kinematic method; Maus et al. 2011). In 2013 and 2017, morphometrics of the
210 studied individual (Id1) were collected using external measurements (when the individual was
211 anesthetised). The geometric model of Crompton *et al.* (1996) was used to estimate the body
212 proportions (segment volume and length) as well as the position of the segment's CoM (i.e. head,
213 trunk, arm, forearm, hand, thigh, shank, foot and tail). Based on these data, we calculated the
214 weighed arithmetic mean of all segments' CoM to estimate the instantaneous position of the BCoM.
215 By using the BCoM displacements, we estimated the variations in kinetic and potential energy during
216 the quadrupedal strides. The kinetic energy (*KE*) is calculated as follows:

$$KE = \frac{1}{2} M_b (V_v^2 + V_{f-a}^2)$$

217 Where M_b is the body mass, V_v is the vertical velocity of the BCoM in the sagittal plane and V_{f-a} is the
 218 velocity in the fore-aft direction. The potential energy (PE) is calculated as follows:

$$PE = M_b g h$$

219 Where g is the gravitational acceleration (9.81 m.s^{-2}) and h is the height of the BCoM. The total
 220 external mass-specific mechanical energy ($W_{ext}; \text{J.kg}^{-1}.\text{m}^{-1}$) is defined as the sum of the positive
 221 increments of the total energy (Δ^+TE) within a cycle, divided by the body mass and the stride length
 222 (SL) of the respective cycle:

$$W_{ext} = \frac{\Delta^+TE}{M_b SL}$$

223 During walking, the BCoM trajectory in relatively large animals (>1kg; Reilly et al. 2007) generally
 224 follows an inverted pendulum movement. In this context, PE and KE fluctuate out-of-phase and
 225 energy exchange between PE and KE is possible. During the rise of the BCoM, energy is converted
 226 from KE to PE, while during the fall PE is converted back into KE. If the amplitudes of both energy
 227 fluctuations are very similar and they fluctuate perfectly out-of-phase, there will be an optimal
 228 energy recovery via the inverted pendulum mechanism (i.e. 100% recovery). Hence, the percentage
 229 of recovery allows us to evaluate the efficiency of the pendular exchange of energy and is estimated
 230 as follows:

$$Recovery (\%) = \frac{\Delta^+PE + \Delta^+KE - \Delta^+TE}{\Delta^+PE + \Delta^+KE} \times 100$$

231 To evaluate the energy exchange mechanism, we calculated two parameters:

232 1) The relative amplitude (RA) between the kinetic and potential energy:

$$RA = \frac{\max(PE) - \min(PE)}{\max(KE) - \min(KE)}$$

233 2) The percentage of the congruity (%C) that is an indication of the phase relationship between PE
 234 and KE:

$$\%C = \frac{\sum_{i=1}^{n-1} [(PE_{i+1} - PE_i)(KE_{i+1} - KE_i) > 0]}{n - 1}$$

235 Where n is the number of values (i.e. 100 data points after stride-normalization, see above). It
 236 measures the proportion of the gait cycle during which both energies change similarly in direction
 237 (Ahn et al. 2004). A perfect energy exchange via the inverted pendulum mechanism (i.e. 100%
 238 recovery) should result in RA=1 and %C=0.

239 *sEMG*

240 We first visually checked the signals to ensure the absence of abnormalities and artefacts. We used
241 MATLAB (R2019a) to analyse, filter and create an envelope of the EMG signals (see the
242 supplementary material for an evaluation of different methods, Figure A). The following successive
243 steps were applied: Band-pass 4th order Butterworth filter (5Hz to 500Hz), centred, rectified (full-
244 wave), low-pass 4th order Butterworth filter (10Hz), rectified (full-wave) [*Matlab script* is available in
245 supplementary material]. We then applied a cubic spline interpolation over a time base with 200
246 points in order to stride-normalized the individual quadrupedal cycles. This provides an envelope of
247 the muscular activity pattern on which we then applied different statistical analyses (see below). Each
248 individual muscle amplitude was also normalized per day of experiment based on the maximum peak
249 contraction value of the set of quadrupedal walking sequences. Due to these treatments, we can
250 average the multiple strides per individual.

251 **Statistics**

252 We proceeded with two analyses: 1) interindividual differences (Id1 *versus* Id2; Table 1) when walking
253 quadrupedally on the ground using the typical DSDC gait; 2) the effect of gait (diagonal *versus* lateral)
254 and substrate (ground *versus* branch). For both analyses, the stride represents the independent
255 statistical unit. Given the small sample size and the heterogeneity, we applied exact (nonparametric)
256 tests: the *Permutation tests* for independent samples.

257 (1) Duty factor, dimensionless stride length and dimensionless stride frequency (and duration)
258 were compared between individuals using *Permutation tests* for independent samples and
259 were regressed against dimensionless speed; the Pearson correlation (r) allowed us to test for
260 significant relationships.

261 (2) Differences in angle average values over a stride are tested between diagonal walking on the
262 ground and diagonal walking on the branch, and diagonal walking on the ground and lateral
263 walking on the ground using *Permutation tests* for independent samples, as well as the range
264 of motion (angle amplitude over a stride), the spatiotemporal parameters (duty factor, stride
265 length, stride duration, speed) and the CoM mechanics (%C, RA, Recovery, W_{ext}).

266 In order to evaluate potential differences between the walking contexts, we divided the EMG signals
267 into 4 phases of equal duration, representing 25% of the cycle duration. The numerical integration of
268 these different phases allowed us to estimate the proportion of EMG activation per phase and its
269 distribution across phases. We conducted a Chi-square test of independence (χ^2) to assess whether
270 there is a significant relationship between the distribution of the activation pattern between

271 individuals (1), and within individual for the different contexts studied (2), i.e. walking on the ground
272 using a diagonal sequence, walking on a branch using a diagonal sequence and walking on the ground
273 using a lateral sequence. Because the data collected in 2017 were obtained the same day on the
274 same individual, we can also compare for this specific day and individual the maximal activation
275 values between gaits and substrates using *Permutation* tests for independent samples. The statistics
276 were conducted using the software for Exact nonparametric inference StatXact 3.1 (Cytel, Inc.,
277 Cambridge, MA). The significance threshold was set at $P < 0.05$.

278 **RESULTS**

279 *Average kinematics*

280 The data used here are for Id1, 15/12/2017 (diagonal/ground n=12; Table 1).

281 Time plots of the hind limb and forelimb joint and segment angles are shown on the figures 3 and 4,
282 respectively. During baboon quadrupedal walking, the hip extends gradually during the stance phase
283 up to $\sim 90^\circ$. It flexes rapidly during the swing phase until it reaches $\sim 50^\circ$ and remains in a constant
284 position at the end of the swing phase just before the foot touches the ground and while the knee is
285 extending. The knee starts flexing slowly during the stance phase and reaches a plateau around mid-
286 stance, but the flexion increases rapidly just before lift-off when the ankle is rapidly extending from
287 65° to 90° . The swing phase is characterized by a rapid flexion of the knee up to 90° during one third
288 of the swing phase and then by a rapid extension until reaching 140° at touch-down. The ankle shows
289 the same pattern as the knee but is slightly delayed. The trunk angle is maintained around 3° on
290 average and remains stable during the quadrupedal stride, the movement amplitude is $\sim 7^\circ$. The
291 shoulder shows a reverse pattern compared to the hip, it flexes gradually during the stance phase of
292 the forelimb until reaching $\sim 40^\circ$ and increases during the swing phase until 80° . The range of motion
293 of the humerus is 39° while the amplitude of the thigh (femur) is 44° . The elbow flexes during the
294 beginning of the swing phase from $\sim 130^\circ$ to $\sim 90^\circ$ and then extends during the second part of the
295 swing phase up to 120° . It increases slowly during the stance phase, but it reaches a plateau around
296 mid-stance, as also observed in the knee. The end of the stance phase is characterized by an
297 extension of the elbow from 130° to 140° . The wrist shows an extreme extension around 220° in the
298 last third of the stance phase that precedes an important roll off before lift-off. The wrist flexes until
299 $\sim 100^\circ$ and then extends again in preparation of touch-down at $\sim 180^\circ$. The high wrist extension
300 corresponds to the typical digitigrade hand posture in baboon and the wrist dorsiflexes gradually
301 during the two third of the stance phase until reaching an extreme extension when the ipsilateral
302 hindlimb touches down.

303 *Average BCoM mechanics*

304 The data used here are for Id1, 15/12/2017 (diagonal/ground n=12) and 04/07/2013
 305 (diagonal/ground n=3).

306 In our sample, the recovery rates of energy are at 57% on average when the walking speed is under
 307 $0.9 \text{ m}\cdot\text{s}^{-1}$ and tend to decrease at higher speed (Fig. 5A). Note, that although we provided a linear
 308 regression model for this relationship, a second-degree polynomial might be a better fit for the data
 309 ($R^2=0.34$ vs $R^2=0.26$ for the linear model). A broader speed range would enable confirmation of the
 310 linear or the upside-down U-shaped relationship between the recovery rates and speed in baboons.
 311 The recovery rates are significantly negatively correlated with the congruity, i.e. the more the
 312 energies are fluctuating out-of-phase, the better the recovery is (Fig. 5B). The percentage of recovery
 313 is also significantly correlated with the limb phase. A limb phase value closer to 0.55 corresponds to a
 314 higher level of recovery. There is no relationship between the recovery rates and the relative
 315 amplitude of the kinetic and potential energy.

316 *Interindividual differences*

317 The data used here are for Id1, 07/2013 (n=3+9) and for Id2, 12/2013 (n=19; see Table 1).

318 **Spatio-temporal parameters** Table 2 shows the average values of the spatio-temporal parameters for
 319 walking quadrupedally at comfort speed on the ground using DSDC gait per individual. The two
 320 individuals studied adjust their spatio-temporal parameters the same way according to speed (see
 321 Figure B in the supplementary material). Both individuals modulate their walking pattern by altering
 322 both their frequency and stride length. Individual 1 tends to increase walking speed mainly by
 323 increasing stride frequency (Id1: slope=0.12 ; Id2: slope=0.04), whereas individual 2 increases speed
 324 mainly by increasing stride length (Id1: slope=3.6; Id2: slope=5.7). The duty factor is significantly
 325 greater in Id1 than in Id2, although the absolute difference is small (67% and 64%, respectively,
 326 *Permutation test*: 3.538, $P=0.0001$). Within the limited speed range observed, the duty factor is not
 327 significantly related to speed for any of the individuals studied. The dimensionless stride length is
 328 longer in Id2 compared to Id1 (4.76 and 4.22, respectively, *Permutation test*: -3.108, $P=0.0004$).

TABLE 2. *Spatio-temporal parameters of steady quadrupedal walking for diagonal sequences on the ground per individual*

	n=12 (Id1)		n=19 (Id2)		<i>P value</i>
	Mean	SD	Mean	SD	Id1 vs Id2
Cycle duration (s)	0.89	0.05	0.95	0.03	0.0029
Stride frequency (1/s)	1.13	0.07	1.05	0.04	0.0024

Stride length (m)	0.68	0.04	0.81	0.05	0.0001
Speed (m.s⁻¹)	0.76	0.07	0.85	0.07	0.0116
Dimensionless values					
Duty factor (%)	67	1	64	1	0.0001
Cycle duration	6.98	0.39	7.25	0.25	ns
Stride frequency	0.14	0.008	0.14	0.005	ns
Stride length	4.22	0.26	4.76	0.30	0.0004
Speed	0.61	0.05	0.66	0.05	ns

ns: not significant

329 **Muscular activity** The bursting EMG patterns are very consistent between the two individuals (Fig. 6).
330 The *gluteus medius* (hip extensor and rotator muscle), the *biceps femoris* (hip extensor and knee
331 flexor), the *gastrocnemius* (ankle extensor muscle) and the *peroneus* (foot evtor muscle) were
332 active at the beginning of the stance phase. The maximum burst activity is approximately 25% of the
333 stance phase, i.e. when the right hind limb is still in a protracted posture and when the (contralateral)
334 left hind limb starts to swing and the left forelimb touches the ground. The *rectus femoris* (hip flexor
335 and knee extensor) shows a reverse pattern with a burst of activity when the limb starts to be
336 retracted, and the knee is maintained around 120°. It is approximately at 75% of the stance phase
337 and corresponds to the (contralateral) left hind limb touching the ground. There is also a certain level
338 of recorded activation of the *rectus femoris* in Id1, at the beginning of the stance phase, when the
339 *gluteus medius*, the *biceps femoris* and the *gastrocnemius* are very active. The distinct activation
340 pattern of the *rectus femoris* is the only significant difference found between the two individuals
341 ($\chi^2=12$, $df=3$, $P=0.0069$). While the activity of the muscles located in the thigh show very short
342 bursting patterns, the burst activity of the *gastrocnemius* and *peroneus* remain active during a longer
343 period of the stance phase, i.e. until the touch-down of the left hind limb. The *tibialis anterior*
344 (dorsiflexion of the foot and inversion) starts its activity at the very end of the stance phase, just after
345 the (ipsilateral) right forelimb touch-down and shows a burst of activity just after the right hind limb
346 lift-off when the ankle is rapidly flexed. Its activity then decreases during the second period of the
347 swing phase. There is no activity of the *gluteus medius*, *rectus femoris*, *biceps femoris*, *peroneus* and
348 *gastrocnemius* during the swing phase, but the *biceps femoris* and *gastrocnemius* appear to start
349 their activity at the very end of the swing phase, in preparation of the touch-down.

350 *Variations around the quadrupedal gait: effects of gait and substrate*

351 The data used here are for Id1, 15/12/2017 (diagonal/ground n=12, lateral/ground n=2,
352 diagonal/branch n=6), and to increase the sample for the lateral walking gait, also for Id1, 04/07/2013
353 (lateral/ground n=2; see Table 1).

354 **Spatio-temporal parameters and BCoM mechanics** Table 3 shows the average values of the
 355 spatiotemporal parameters for walking quadrupedally on the ground using diagonal sequences (DS-
 356 G), for walking quadrupedally on the branch using diagonal sequences (DS-B) and for walking
 357 quadrupedally on the ground using lateral sequences (LS-G). We observed a significant difference in
 358 stride frequency (and duration) between diagonal and lateral gaits (1.26Hz and 1.44Hz, respectively,
 359 Permutation test: 2.193, $P=0.0209$) as well as in the % of congruity of the BCoM (38.7% and 53.6%,
 360 respectively, Permutation test: -2.272, $P=0.0159$). There is a significant difference in stride length and
 361 speed when walking on the ground compared to the branch (stride length: 0.73m and 0.66m,
 362 respectively, Permutation test: 2.277, $P=0.0197$; speed: $0.92\text{m}\cdot\text{s}^{-1}$ and $0.79\text{m}\cdot\text{s}^{-1}$, respectively,
 363 Permutation test: 2.089, $P=0.0335$).

TABLE 3. Spatio-temporal parameters and BCoM mechanics of steady quadrupedal walking in different substrate and gait contexts

	DS-G (n=12)		LS-G (n=4)		DS-B (n=6)		P value	
	Mean	SD	Mean	SD	Mean	SD	DS-G vs LS-G	DS-G vs DS-B
Spatio-temporal parameters								
Cycle duration (s)	0.80	0.04	0.71	0.07	0.84	0.07	0.0209	ns
Stride frequency (1/s)	1.26	0.06	1.44	0.15	1.2	0.1	0.0209	ns
Stride length (m)	0.73	0.04	0.71	0.05	0.66	0.03	ns	0.0197
Speed ($\text{m}\cdot\text{s}^{-1}$)	0.92	0.08	1.01	0.12	0.79	0.10	ns	0.0335
Duty factor (%)	64	2	65	2	66	2	ns	ns
BCoM mechanics								
Recovery rates (%)	42.8	9.6	27.9	9.8	32.3	8.6	0.0566 ¹	0.0907
Congruity (%)	38.7	7	53.6	10	46	12	0.0159	ns
Relative amplitude	0.86	0.26	0.41	0.13	0.78	0.27	0.0648	ns
External energy ($\text{J}\cdot\text{kg}^{-1}\cdot\text{m}^{-1}$)	0.33	0.08	0.33	0.05	0.36	0.10	ns	ns

Significant values are indicated in bold

¹values close to the significance threshold (i.e. $0.05 < P < 0.1$) are also indicated

364 **Kinematics** The ankle angle is more extended and the shank angle is more flexed during lateral gait
 365 compared to diagonal gait (ankle: 82.1° and 76.4° , respectively, Permutation test: -2.509, $P=0.0121$;
 366 shank: 51.4° and 53.7° , respectively, Permutation test: 2.157, $P=0.0247$). The range of motion (ROM)
 367 of the knee angle is greater during diagonal walking compared to lateral walking (51.5° and 47.3° ,
 368 respectively, Permutation test: 1.914, $P=0.0247$).

369 On the branch, the baboon increases the ankle extension and the range of motion of the ankle as
 370 well as the shank extension compared to the ground (ankle: 82.3° and 76.4° , respectively,

371 *Permutation test*: -3.165, $P=0.0004$; ankle ROM: 44.9° and 38.3°, respectively, *Permutation test*: -2.08,
372 $P=0.0339$; shank: 56.6° and 53.7°, respectively, *Permutation test*: -2.79, $P=0.0023$). The range of
373 motion of the trunk angle is reduced on the branch compared to the ground (4° and 6.3°,
374 respectively, *Permutation test*: 2.862, $P=0.0015$). In the forelimb, the shoulder angle is kept more
375 extended on the branch compared to the ground and the wrist is more dorsiflexed (shoulder: 58.4°
376 and 55.3°, respectively, *Permutation test*: -2.09, $P=0.0326$; wrist: 187° and 180.8°, respectively,
377 *Permutation test*: -2.53, $P=0.0081$). Figure C (in the supplementary material) shows the average
378 pattern for each joint and segment angle studied in each gait and substrate context.

379 **Muscular activity** The bursting EMG profiles are very consistent across gaits and substrates (Fig. 7).
380 There is no difference between the lateral and the diagonal sequences performed on the ground **as**
381 **far as the bursting EMG profiles are concerned**. But the maximal burst of activity of the *biceps*
382 *femoris*, *gastrocnemius* and *tibialis anterior* significantly increase in lateral sequences (*Permutation*
383 *test*: -1.909, $P=0.0467$; *Permutation test*: -2.042, $P=0.0379$ and *Permutation test*: -2.595, $P=0.0055$,
384 respectively).

385 With regard to the quadrupedal strides performed on the ground and on the branch, we observe a
386 significant difference of the activation pattern at the level of the *peroneus* ($\chi^2=10.62$, $df=3$, $P=0.0137$).
387 While the activity of the *peroneus* is concentrated at the beginning of the stance phase when the
388 baboon is walking steadily on the ground, its activity is kept during all the stance phase when walking
389 on the branch. Furthermore, the maximal activity of the *peroneus* is significantly higher on the branch
390 than on the ground (*Permutation test*: -2.858, $P=0.0022$). The maximal burst of activity of the *rectus*
391 *femoris* is significantly lower on the branch (*Permutation test*: 2.106, $P=0.0231$).

392 **DISCUSSION**

393 The present study aims to explore the quadrupedal walking pattern of baboons using different levels
394 of analysis, via limb and body kinematics (also used to estimate the dynamics of the BCoM) and
395 muscular activity. Overall, our study shows that the dynamics of the BCoM in a baboon walking
396 quadrupedally on the ground using its preferred walking gait (DSDC) is effective **and can be**
397 energetically efficient. On the other hand, walking on a branch appears to give priority to stability, but
398 how it affects efficiency **requires further exploration**. In addition, walking using the LSLC **gait appears**
399 **to** increase muscular effort and may reduce the potential for high recovery rates in baboons.
400 Importantly, although our study supports specific assumptions about stability and efficiency in non-
401 human primates, further data including a larger sample size are required.

402 *Walking on the ground using DSDC gait*

403 Overall, the patterns of muscular activation during steady quadrupedal walking in baboons are
404 consistent within and between individuals (Figure 6B shows an overview of the muscular activity
405 pattern during quadrupedal walking). The phasic activities of the six recorded muscles are very
406 similar to the muscular activity profile described in macaques (Courtine et al. 2005; Higurashi et al.
407 2019). Furthermore, despite differences in the footfall pattern between non-primate quadrupedal
408 mammals (lateral sequences) and non-human primates (diagonal sequences), the activity pattern of
409 the hind limb muscles in baboons is very similar to the one observed in other primates such as
410 chimpanzees, spider monkeys, macaques, and lemurs (Ishida et al. 1974; Kimura et al. 1979; Larson &
411 Stern 2009), as well as in dogs (Deban et al. 2012; Goslow et al. 1981) and cats (Rasmussen et al.
412 1978). Therefore, we can assume that the basic functions of the muscles for retracting and
413 protracting the limbs, as well as to support the body against gravity and inertial forces are conserved
414 across groups.

415 We first hypothesized that, given the "cursorial" adaptations of baboons (e.g. Druelle et al. 2017a;
416 Patel & Polk 2010; Raichlen 2004), they should be able to make use of an inverted-pendulum
417 mechanism when walking steadily on the ground. Our results support this hypothesis as we observed
418 that KE and PE are mainly fluctuating out-of-phase (congruity = 39%) during normal quadrupedal
419 walking using DSDC gaits. The recovery rates observed in baboon in this study (22-84%) cover an
420 important range of variation compared to other specialized quadrupeds such as dogs (50-70%; Griffin
421 et al. 2004), but these are close to the range of values available for non-human primates, such as the
422 ring-tailed lemurs and the capuchin monkeys (35-71% and 11-65%, respectively during quadrupedal
423 walking; O'Neill & Schmitt 2012; Demes & O'Neill 2013). Griffin et al. (2004) developed a model
424 showing that the pendulum-like centre of mass movements in quadrupedal animals is a combination
425 of both inverted pendulums around the pectoral and pelvic girdle. These pendulums are directly
426 influenced by the footfall pattern and body mass distribution. For example, a body centre of mass
427 located at mid-trunk coupled to a forelimb that lags behind the hindlimb by 25% would result in a flat
428 trajectory of the BCoM (Griffin et al. 2004). Baboons have a BCoM positioned at mid-trunk compared
429 to dogs that have a cranially positioned BCoM (Druelle et al. 2019), hence baboons may rely on limb
430 phase only to produce "optimal" fluctuations of their BCoM. In the present study, we found that the
431 ipsilateral forelimb lagged behind the hindlimb by 61% in average (min: 54%, max: 69%) and there is a
432 significant relationship between the recovery rates and the limb phase (i.e. the lags between fore-
433 and hindlimbs; see Figure 5C). These results support the model of Griffin et al. (2004), but it does not
434 support the "reduced cost zone" of 65-72% estimated recently by Miller et al. (2019) for non-human
435 primates. However, note that, as recognized by the latter, body mass distribution can also affect the
436 model and specific primate conformation is likely to shift the "reduced cost zone" of the footfall

437 timing. In addition, given the small size of our sample, our results should be carefully considered
438 before rejecting previous assumptions.

439 Our results, in addition to the ones provided by O'Neill & Schmitt (2012) and Demes & O'Neill (2013),
440 do not support the hypothesis of Ogihara et al. (2012) suggesting that diagonal sequence gaits
441 impede good recovery rates in primates. The baboon appears, however, much more efficient than the
442 macaque (Ogihara et al. 2012) when walking on the ground. As previously suggested (Druelle et al.
443 2016), macaques may be less equipped for quadrupedal walking than baboons. Because baboons
444 commonly travel at least 3.5 km per day, while macaques move less than 1.5 km (Garland 1983), the
445 specific ecological requirements of baboons may have shaped these species into more efficient
446 walkers (i.e. higher potential for relying on inverted-pendulum strategies) than macaques. Given the
447 ecological niche of olive baboons and their large home range (Garland 1983; Henzi et al. 1992; Isbell
448 et al. 1998; Pebsworth et al. 2012), they should be under strong selection for walking efficiency
449 (Druelle et al. 2017a). This could also be the case for the ring-tailed lemurs and the capuchin monkeys
450 that both exhibit good recovery rates during quadrupedal walking (O'Neill & Schmitt 2012; Demes &
451 O'Neill 2013).

452 *Influence of different gait and substrate contexts*

453 When walking on a branch, an inherent instability (rolling and pitching moments) is in action. Our
454 second hypothesis stipulated that when walking on a branch, kinematical adjustments should reduce
455 the vertical oscillations of the centre of mass (Gálvez-López et al. 2011; Schmitt 1999) and in this way
456 give priority to stability upon efficiency (but see Schmitt 2011). It has been shown that animals
457 increase their stability on arboreal substrates through **employing** strategies that reduce the
458 oscillations of their BCoM (Gálvez-López et al. 2011). However, these strategies can be of a different
459 kind. For instance, while cats (medium-sized, ≈4.4kg) make use of slower speeds and shorter swing
460 phase durations on a narrow runway, dogs (large-sized, ≈28kg), on the other hand, rely on high-speed
461 locomotion and high frequency to gain dynamic stability (Gálvez-López et al. 2011). The adjustments
462 observed in the olive baboon (13.5kg in the present study) when walking on a (suspended, non-
463 bending) branch show a decrease in stride length and speed, a decrease in the movement amplitude
464 of the trunk and a trend towards a longer relative contact time. There is also an increase in ankle and
465 wrist extension that results from a slight external rotation of the distal limb segments to fit the
466 rounded shape of the substrate. The decrease in trunk range of motion may result in part from the
467 shorter stride length and thus from the lower speed, as well as from the shoulder that is kept more
468 extended on the branch. More in-phase fluctuations of the KE and PE (congruity = 46%) are also
469 observed compared to the walk on the ground. These adjustments (certainly closer to the cat

470 strategy) reduce the vertical oscillations of the BCoM, and with the increase activity of the *peroneus*
471 (increasing torque generation), meet the balance control requirements. This general strategy may
472 reduce the possibility to rely on an efficient inverted pendulum-like exchange of energy, but we did
473 not observe a direct significant difference in the recovery rates. The baboon thus appears to adjust its
474 movement and to increase the control in the distal segment to gain stability, but more data are
475 required to assess how much this strategy influences the efficiency. Interestingly, a previous study
476 showed that in *Lemur catta*, walking on a raised horizontal pole does not significantly affect the
477 energetic recovery (Schmitt 2011). Furthermore, limb interference is important during diagonal
478 walking on the ground. The baboons move their right hind limb on the right (or left) side of their right
479 forelimb, while the left hindlimb moves on the right (or left) side of the left forelimb (Fig. 6b). On the
480 branch, there is no space for limb interference and overstriding during walking and the hindlimbs
481 need to be positioned behind the forelimbs at touch-down. This can also contribute to the shorter
482 stride lengths and lower speed observed on the branch.

483 A study on bonobos observed that when they walk on a horizontal arboreal substrate, they reduce
484 their stance phase, take longer strides and reduce the stride frequency (Schoonaert et al. 2016). This
485 strategy appears to be very different from the one used by the baboon in the present study (note that
486 both, the size of the specimens and the substrate diameter are different: 12cm for the bonobos, and
487 16cm in the present study), as well as from the ones used by lemurs and marmosets that all tend to
488 decrease their speed and increase the contact time with the substrate (Franz et al. 2005; Young et al.
489 2016). However, we wonder whether the pole height may also be of importance. For instance, the
490 bonobos were walking on a pole that was positioned approximately 30cm above the ground, hence
491 falling was not really a risk encountered by the animals (Schoonaert et al. 2016). This emphasizes the
492 importance of considering morphological differences, kinematic strategies coupled to risk evaluation
493 among primates for negotiating arboreal substrates [hominoids, cercopithecoids, platyrrhines and
494 lemuriforms all present different morphological features (Fleagle 2013)]. Although balance
495 requirements are shared between animals when walking on a horizontal branch, the ability to meet
496 these demands (controlling pitching, yawing and rolling moments) can be performed in very different
497 ways, i.e. from static to dynamic stability of the BCoM. It is possible that all these strategies allow
498 primates and other mammals to limit the vertical oscillations of the BCoM, given their respective
499 morphology (e.g. Gàlvez-López et al. 2011; Schmitt et al. 2006; Young et al. 2016).

500 Muscular effort is influenced by the footfall pattern (Bishop et al. 2008; Griffin et al. 2004), hence
501 energetic cost is probably an important factor in footfall timings (Miller et al. 2019). We hypothesized
502 that the usual muscle activation pattern observed in diagonal gaits should be altered towards an
503 increased activation of the proximal muscles when the baboon uses the unusual lateral gait on the

504 ground and of the distal muscles (for increasing the control) when it walks on a substrate that
505 imposes higher balance requirements (such as a branch). First, we observed an increased activity of
506 the *biceps femoris*, the *gastrocnemius* and the *tibialis anterior* when walking using LSLC gait on the
507 ground. Second, the *peroneus* activity increases substantially in intensity and duration during the
508 stance phase when walking on the branch. Generally, the *peroneus* is suggested to stabilize the ankle
509 and to be an extensor and evertor of the foot. Boyer et al. (2007) suggested that the *peroneus*
510 (*longus*) is an important muscle for positioning the foot at touchdown and for resisting inversion
511 throughout the stance phase in primates. The activity of the *peroneus* observed in our study when
512 the baboon is walking on the branch is similar to the one of the lemur species walking quadrupedally
513 on large and small poles (Boyer et al. 2007). While it is not strongly active on the ground during
514 diagonal and lateral gaits in baboons, it appears to be specifically recruited for resisting foot inversion
515 during the stance phase on the branch. Our kinematics support this, as we observed an increase in
516 ankle extension (and external rotation). The more outward and everted position of the foot should
517 ensure a better fit between the foot and the substrate, thus increasing friction and allowing
518 transmitting rotating moment (Lammers & Gauntner 2008; Preuschoft 2004).

519 The *biceps femoris* is described as a hip extensor and a knee flexor (Swindler & Wood 1973). It is
520 active during the initial part of the support phase. At touch-down, the limb is in a protracted position
521 and the knee is relatively extended ($\approx 140^\circ$) (Larney & Larson 2004), the *biceps femoris* is, therefore,
522 acting as a thigh (hind limb) retractor by flexing the knee ($\approx 110^\circ$ at midstance) and extending the hip
523 (from 50° to 75° between touch-down and mid-stance). The fact that its activity increases
524 substantially during lateral walking can be directly related to the higher stride frequency (relative
525 stance phase does not change). The increase activity of the *gastrocnemius* and the *tibialis anterior*
526 may also result from the higher stride frequency. A faster retraction and protraction of the limb
527 would require more muscular fibres to be active. Lateral walking also led to an increase extension of
528 the ankle that can be related to the increase activity observed in the *gastrocnemius* and the *tibialis*
529 *anterior*. But the functional reason for this higher extension remains elusive at this stage (note that
530 such an ankle extension in this context also seems to be seen in capuchin monkey; see Figure 2 in
531 Wallace and Demes 2008). On the branch, the stride length decreases as well as the speed and the
532 activity of the *rectus femoris* (for controlling limb retraction) is reduced in this context.

533 CONCLUSION

534 The present study provides new exploratory data on the normal quadrupedal gait pattern in olive
535 baboons. It is also an attempt to better understand the flexibility of the quadrupedal gait in different
536 contexts. Baboons mainly walk quadrupedally on the ground using DSDC gait and our evaluation of

537 the dynamics of the BCoM using kinematics suggests that this is more efficient than walking using the
538 LSLC gait. Also, from a motor perspective, significant increase in muscular activity should result in
539 higher level of oxygen consumption. Hence, the most efficient baboon remains the one walking on
540 the ground, using DSDC gaits (potentially with a tight limb phase: $50\% < LP > 60\%$ and at low speed, but
541 data from a larger speed range are **required** to assess how it influences the energetic recovery rates,
542 i.e., linearly or not). **Moreover**, our data suggest that the use of a different walking gait, or walking on
543 a branch, both result in less efficient forms of locomotion. **Although our analysis on this aspect is**
544 **preliminary**, this emphasizes a possible limitation in the flexibility of the walking pattern when
545 efficiency is the target. In other words, walking economy could be related to a stereotyped, non-
546 flexible pattern, while gait adjustments and flexibility ensure stability in an arboreal habitat. However,
547 further data are required to investigate this hypothesis. As recently claimed, the effect of footfall
548 timings on mechanical stability and mechanical energy exchange on arboreal and terrestrial
549 substrates, as well as the way these competing demands interact (Miller et al. 2019) remains poorly
550 known. It is also possible that these two components do not have the same "time-frame" as
551 mechanical energy exchange should occur within a stride, while mechanical stability can be
552 performed and ensured among multiple strides (Biewener & Daley 2007; Chadwell & Young 2015;
553 Lammers & Gauntner 2008). **Further integrative data including larger sample size are needed to**
554 **better understand the relationships between gait adjustments, BCoM mechanics and muscular**
555 **activity in non-human primates.**

556 Overall, the quadrupedal peculiarities of primates certainly represent biomechanical
557 accommodations to arboreal life and played a crucial role in the early differentiation of primates from
558 other mammals. However, despite these peculiarities, they also share very similar patterns of muscle
559 activation with other quadrupedal mammals, at least when they walk quadrupedally on the ground.
560 This reflects the shared basic functional demands (i.e. support and propulsion) on the hind limbs for
561 quadrupedal locomotion in tetrapods. Finally, the diagonal gait pattern appears to be strongly
562 implemented into the baboon neuromotor system because lateral sequences are likely to result in a
563 direct and significant increase of the energetic costs (at the level of the BCoM mechanics and
564 muscular activity). On the other hand, the diagonal walking gait does not impede good recovery rates
565 in primates.

566

AKNOWLEDGEMENTS

567 We are very grateful to Romain Lacoste and Thomas Brochier, the director and the scientific director,
568 respectively, of the Primatology Station of the CNRS, who provided access and facilities to the
569 animals. We are very grateful to Josie Meaney-Ward who revised and improved the English of the

570 manuscript. We thank the referees for their constructive and detailed comments on the previous
571 versions of the manuscripts. The Technical Platform has been funded by the CNRS-INEE, the sEMG
572 material has been funded by the IBISA platform of the CNRS (Exploration Fonctionnelle Primates).
573 This project is funded by ANR-18-CE27-0010-01 and CNRS-INEE International Research Network IRN-
574 GDRI0870.

575

FIGURE LEGENDS

576 **Figure 1.** Schematic diagram of a baboon walking quadrupedally including the average position of the
577 6 recorded extrinsic muscles (in red). The positioning of the electrodes (connected to their respective
578 wireless battery) for the 6 muscles studied can be seen on the picture under the schematic diagram:
579 1, *gluteus medius* (hip extensor and rotator); 2, *rectus femoris* (hip flexor and knee extensor); 3,
580 *biceps femoris* (hip extensor and knee flexor); 4, *medial gastrocnemius* (plantar flexion and knee
581 flexion), 5; *peroneus* (foot eversion); 6, *tibialis anterior* (dorsiflexion of the foot and inversion).

582 **Figure 2.** Schematic diagram showing the position of the digitized anatomical points, the internal
583 (blue) and external (red) angles measured and the BCoM in the middle of the trunk.

584 **Figure 3.** Average hind limb joint and segment angles (\pm 95% Confidence Interval) for Id1, during
585 quadrupedal walking (DSDC) at comfort speed ($\sim 0.92\text{m}\cdot\text{s}^{-1}$), including the average footfall pattern.
586 The joint and segment angles are measured on the right side. The average footfall pattern at the
587 bottom (gait diagram) shows average stance phases (solid bars) of the right hind limb (RH), left hind
588 limb (LH), right forelimb (RF) and left forelimb (LF). The right hind limb is the limb of reference. It is
589 darker on the gait diagram and the stance phase is indicated on the graphs with a light background.

590 **Figure 4.** Average forelimb joint and segment angles (\pm 95% Confidence Interval) for Id1, during
591 quadrupedal walking (DSDC) at comfort speed ($\sim 0.92\text{m}\cdot\text{s}^{-1}$), including the average footfall pattern.
592 The joint and segment angles are measured on the right side. The average footfall pattern at the
593 bottom (gait diagram) shows average stance phases (solid bars) of the right hind limb (RH), left hind
594 limb (LH), right forelimb (RF) and left forelimb (LF). The right forelimb is the limb of reference. It is
595 darker on the gait diagram and the stance phase is indicated on the graphs with a light background.

596 **Figure 5.** Influence of various walking variables on the recovery rates during quadrupedal locomotion.
597 A significant relationship is found between speed and the recovery rates (A), the congruity of the
598 fluctuations of kinetic and potential energy and the recovery rates (B) and the diagonality and the
599 recovery rates (C), but not between the relative amplitude of the fluctuation of kinetic and potential
600 energy and the recovery rates (D).

601 **Figure 6.** (a) Average EMG profiles of the 6 hind limb muscles considered during steady quadrupedal
602 walking. The activity patterns are stride-normalized and averaged across 12 strides for Id1 (grey) and
603 19 strides for Id2 (blue). The average footfall pattern at the bottom (gait diagram) shows average
604 stance phases (solid bars) of the right hind limb (RH), left hind limb (LH), right forelimb (RF) and left
605 forelimb (LF). The EMG activity was recorded on the right hind limb (darker on the gait diagram). (b)
606 Overview of the muscular activity of the 6 hind limb muscles considered during the stance phase of
607 the quadrupedal stride in Id1. The amount of muscular activity is based on the average profile
608 observed in (a) and is divided in 4 levels of activation. Six events are represented: Right Hind limb
609 Touch-Down (RH TD), Left Hind limb Lift-Off (LH LO) + Left Forelimb Touch-Down (LF TD), Right
610 Forelimb Lift-Off (RF LO), Left Hind limb Touch-Down (LH TD), Right Forelimb Touch-Down (RF TD) and
611 Right Hind limb Lift-Off (RH LO).

612 **Figure 7.** Average EMG profiles of the 6 hind limb muscles considered during steady quadrupedal
613 walking for Id1 (recorded in 2017, see Table 1). The activity patterns are stride-normalized and
614 averaged across 12 strides when walking on the ground (green), 4 strides when walking using lateral
615 sequences (dark blue) and 6 strides when walking on the branch (light blue). The average footfall
616 pattern at the bottom (gait diagram) shows average stance phases (solid bars) of the right hind limb
617 (RH), left hind limb (LH), right forelimb (RF) and left forelimb (LF). The EMG activity was recorded on
618 the right hind limb.

619

REFERENCES

- 620 Aerts, P., Van Damme, R., Van Elsacker, L. & Duchene, V. 2000 Spatio-temporal gait characteristics of
621 the hind-limb cycles during voluntary bipedal and quadrupedal walking in bonobos (*Pan*
622 *paniscus*). *American journal of physical anthropology* **111**, 503-517.
- 623 Ahn, A. N., Furrow, E. & Biewener, A. A. 2004 Walking and running in the red-legged running frog,
624 *Kassina maculata*. *Journal of Experimental Biology* **207**, 399-410.
- 625 Alexander, R. M. 1991a Elastic mechanisms in primate locomotion. *Zeitschrift für Morphologie und*
626 *Anthropologie*, 315-320.
- 627 Alexander, R. M. 1991b Energy-saving mechanisms in walking and running. *Journal of Experimental*
628 *Biology* **160**, 55-69.
- 629 Anvari, Z., Berillon, G., Asgari Khaneghah, A., Grimaud-Herve, D., Moulin, V. & Nicolas, G. 2014
630 Kinematics and spatiotemporal parameters of infant-carrying in olive baboons. *American*
631 *Journal of Physical Anthropology* **155**, 392-404.
- 632 Berillon, G., D'Août, K., Daver, G., Dubreuil, G., Multon, F., Nicolas, G., Villetanet, B. & Vereecke, E. E.
633 2011 In What Manner Do Quadrupedal Primates Walk on Two Legs? Preliminary Results on
634 Olive Baboons (*Papio anubis*). In *Primate Locomotion* (ed. L. Barrett), pp. 61-82: Springer New
635 York.
- 636 Berillon, G., Daver, G., D'Août, K., Nicolas, G., de la Villetanet, B., Multon, F., Digrandi, G. & Dubreuil,
637 G. 2010 Bipedal versus Quadrupedal Hind Limb and Foot Kinematics in a Captive Sample of
638 *Papio anubis*: Setup and Preliminary Results. *International Journal of Primatology* **31**, 159-
639 180.

640 Biewener, A. A. 1989 Scaling body support in mammals: limb posture and muscle mechanics. *Science*
641 **245**, 45-48.

642 Biewener, A. A. & Daley, M. A. 2007 Unsteady locomotion: integrating muscle function with whole
643 body dynamics and neuromuscular control. *Journal of Experimental Biology* **210**, 2949-2960.

644 Bishop, K. L., Pai, A. K. & Schmitt, D. 2008 Whole Body Mechanics of Stealthy Walking in Cats. *PLoS*
645 *one* **3**, e3808.

646 Boyer, D. M., Patel, B. A., Larson, S. G. & Stern Jr, J. T. 2007 Telemetered electromyography of
647 peroneus longus in *Varecia variegata* and *Eulemur rubriventer*: implications for the functional
648 significance of a large peroneal process. *Journal of Human Evolution* **53**, 119-134.

649 Cartmill, M. 1974 Pads and claws in arboreal locomotion. *Primate locomotion*, 45-83.

650 Cartmill, M., Brown, K., Atkinson, C., Cartmill, E. A., Findley, E., Gonzalez-Socoloske, D., Hartstone-
651 Rose, A. & Mueller, J. 2020 The gaits of marsupials and the evolution of diagonal-sequence
652 walking in primates. *American Journal of Physical Anthropology* **171**, 182-197.

653 Cartmill, M., Lemelin, P. & Schmitt, D. 2002 Support polygons and symmetrical gaits in mammals.
654 *Zoological Journal of the Linnean Society* **136**, 401-420.

655 Cavagna, G. A., Heglund, N. C. & Taylor, C. R. 1977 Mechanical work in terrestrial locomotion: two
656 basic mechanisms for minimizing energy expenditure. *American Journal of Physiology-
657 Regulatory, Integrative and Comparative Physiology* **233**, R243-R261.

658 Chadwell, B. A. & Young, J. W. 2015 Angular momentum and arboreal stability in common marmosets
659 (*Callithrix jacchus*). *American Journal of Physical Anthropology* **156**, 565-576.

660 Courtine, G. g., Roy, R. R., Hodgson, J., McKay, H., Raven, J., Zhong, H., Yang, H., Tuszynski, M. H. &
661 Edgerton, V. R. 2005 Kinematic and EMG determinants in quadrupedal locomotion of a non-
662 human primate (Rhesus). *Journal of neurophysiology* **93**, 3127-3145.

663 Crompton, R. H., Li, Y., Alexander, R. M., Wang, W. & Gunther, M. M. 1996 Segment inertial properties
664 of primates: New techniques for laboratory and field studies of locomotion. *American Journal
665 of Physical Anthropology* **99**, 547-570.

666 De Luca, C. J., Gilmore, L. D., Kuznetsov, M. & Roy, S. H. 2010 Filtering the surface EMG signal:
667 Movement artifact and baseline noise contamination. *Journal of Biomechanics* **43**, 1573-
668 1579.

669 Deban, S. M., Schilling, N. & Carrier, D. R. 2012 Activity of extrinsic limb muscles in dogs at walk, trot
670 and gallop. *Journal of Experimental Biology* **215**, 287-300.

671 Demes, B., Larson, S., Stern, J., Jungers, W., Biknevicius, A. & Schmitt, D. 1994 The kinetics of primate
672 quadrupedalism: "hindlimb drive" reconsidered. *Journal of Human Evolution* **26**, 353-374.

673 Demes, B. & O'Neill, M. C. 2013 Ground reaction forces and center of mass mechanics of bipedal
674 capuchin monkeys: Implications for the evolution of human bipedalism. *American Journal of
675 Physical Anthropology* **150**, 76-86.

676 Dietz, V. 2002 Do human bipeds use quadrupedal coordination? *Trends in Neurosciences* **25**, 462-467.

677 Druelle, F., Aerts, P. & Berillon, G. 2016 Effect of body mass distribution on the ontogeny of positional
678 behaviors in non-human primates: Longitudinal follow-up of infant captive olive baboons
679 (*Papio anubis*). *American Journal of Primatology* **78**, 1201-1221.

680 Druelle, F., Aerts, P., D'Août, K., Moulin, V. & Berillon, G. 2017a Segmental morphometrics of the olive
681 baboon (*Papio anubis*): a longitudinal study from birth to adulthood. *Journal of Anatomy* **230**,
682 805-819.

683 Druelle, F., Aerts, P., Ngawolo, J. C. B. & Narat, V. 2020 Impressive Arboreal Gap-Crossing Behaviors in
684 Wild Bonobos, *Pan paniscus*. *International Journal of Primatology*, 1-12.

685 Druelle, F., Berillon, G. & Aerts, P. 2017b Intrinsic limb morpho-dynamics and the early development
686 of interlimb coordination of walking in a quadrupedal primate. *Journal of Zoology* **301**, 235-
687 247.

688 Druelle, F., Berthet, M. & Quintard, B. 2019 The body center of mass in primates: Is it more caudal
689 than in other quadrupedal mammals? *American Journal of Physical Anthropology* **169**, 170-
690 178.

- 691 Druelle, F., Young, J. & Berillon, G. 2018 Behavioral implications of ontogenetic changes in intrinsic
692 hand and foot proportions in olive baboons (*Papio Anubis*). *American Journal of Physical*
693 *Anthropology* **165**, 65-76.
- 694 Dunbar, D. C. & Badam, G. L. 2000 Locomotion and posture during terminal branch feeding.
695 *International Journal of Primatology* **21**, 649-669.
- 696 Fleagle, J. G. 2013 *Primate Adaptation and Evolution: 3rd Edn*: Academic Press.
- 697 Foster, A. D., Raichlen, D. A. & Pontzer, H. 2013 Muscle force production during bent-knee, bent-hip
698 walking in humans. *Journal of Human Evolution* **65**, 294-302.
- 699 Franz, T. M., Demes, B. & Carlson, K. J. 2005 Gait mechanics of lemurid primates on terrestrial and
700 arboreal substrates. *Journal of Human Evolution* **48**, 199-217.
- 701 Gálvez-López, E., Maes, L. D. & Abourachid, A. 2011 The search for stability on narrow supports: an
702 experimental study in cats and dogs. *Zoology* **114**, 224-232.
- 703 Garland, T. J. 1983 Scaling the Ecological Cost of Transport to Body Mass in Terrestrial Mammals. *The*
704 *American Naturalist* **121**, 571-587.
- 705 Grand, T. I. 1977 Body weight: its relation to tissue composition, segment distribution, and motor
706 function. I. Interspecific comparisons. *American Journal of Physical Anthropology* **47**, 211-
707 239.
- 708 Gebo, D. L. & Sargis, E. J. 1994 Terrestrial adaptations in the postcranial skeletons of guenons.
709 *American Journal of Physical Anthropology* **93**, 341-371.
- 710 Goslow, G., Seeherman, H., Taylor, C., McCutchin, M. & Heglund, N. 1981 Electrical activity and
711 relative length changes of dog limb muscles as a function of speed and gait. *Journal of*
712 *Experimental Biology* **94**, 15-42.
- 713 Grand, T. I. 1977 Body weight: its relation to tissue composition, segment distribution, and motor
714 function. I. Interspecific comparisons. *American Journal of Physical Anthropology* **47**, 211-
715 239.
- 716 Griffin, T. M., Main, R. P. & Farley, C. T. 2004 Biomechanics of quadrupedal walking: how do four-
717 legged animals achieve inverted pendulum-like movements? *Journal of Experimental Biology*
718 **207**, 3545-3558.
- 719 Hamrick, M. W. 2001 Primate origins: evolutionary change in digital ray patterning and segmentation.
720 *Journal of Human Evolution* **40**, 339-351.
- 721 Hashimoto, T., Ueno, K., Ogawa, A., Asamizuya, T., Suzuki, C., Cheng, K., Tanaka, M., Taoka, M.,
722 Iwamura, Y. & Suwa, G. 2011 Hand before foot? Cortical somatotopy suggests manual
723 dexterity is primitive and evolved independently of bipedalism. *Phil. Trans. R. Soc. B* **368**,
724 20120417.
- 725 Hayama, S., Chatani, K. & Nakatsukasa, M. 1994 The digitigrade hand and terrestrial adaptation in
726 Japanese macaques. *Anthropological Science* **102**, 115-125.
- 727 Henzi, S., Byrne, R. & Whiten, A. 1992 Patterns of movement by baboons in the Drakensberg
728 mountains: primary responses to the environment. *International Journal of Primatology* **13**,
729 601-629.
- 730 Higurashi, Y., Maier, M. A., Nakajima, K., Morita, K., Fujiki, S., Aoi, S., Mori, F., Murata, A. & Inase, M.
731 2019 Locomotor kinematics and EMG activity during quadrupedal versus bipedal gait in the
732 Japanese macaque. *Journal of neurophysiology* **122**, 398-412.
- 733 Hildebrand, M. 1967 Symmetrical gaits of primates. *American Journal of Physical Anthropology* **26**,
734 119-130.
- 735 Hirasaki, E., Kumakura, H. & Matano, S. 1995 Electromyography of 15 limb muscles in Japanese
736 macaques (*Macaca fuscata*) during vertical climbing. *Folia Primatologica* **64**, 218-224.
- 737 Hof, A. L. 1996 Scaling gait data to body size. *Gait & posture* **4**, 222-223.
- 738 Hultborn, H., Petersen, N., Brownstone, P. & Nielsen, J. 1993 Evidence of fictive spinal locomotion in
739 the marmoset (*Callithrix jacchus*). In *Soc Neurosci Abstr*, vol. 19.
- 740 Hunt, K. D. 2016 Why are there apes? Evidence for the co-evolution of ape and monkey
741 ecomorphology. *Journal of Anatomy* **228**, 630-685.

- 742 Hunt, K. D., Cant, J., Gebo, D., Rose, M., Walker, S. & Youlatos, D. 1996 Standardized descriptions of
743 primate locomotor and postural modes. *Primates* **37**, 363-387.
- 744 Hylander, W. L. & Johnson, K. R. 1993 Modelling relative masseter force from surface
745 electromyograms during mastication in non-human primates. *Archives of oral biology* **38**,
746 233-240.
- 747 Isbell, L. A., Pruetz, J. D., Lewis, M. & Young, T. P. 1998 Locomotor activity differences between
748 sympatric patas monkeys (*Erythrocebus patas*) and vervet monkeys (*Cercopithecus aethiops*):
749 implications for the evolution of long hindlimb length in Homo. *American Journal of Physical*
750 *Anthropology: The Official Publication of the American Association of Physical*
751 *Anthropologists* **105**, 199-207.
- 752 Ishida, H., Kimura, T. & Okada, M. 1974 Patterns of bipedal walking in anthropoid primates. In
753 *Proceedings of the 5th congress of the International Primatological Society, 1974*, pp. 287-
754 301: Japan Science Press.
- 755 Jungers, W. L. & Anapol, F. C. 1985 Interlimb coordination and gait in the brown lemur (*Lemur fulvus*)
756 and the talapoin monkey (*Miopithecus talapoin*). *American Journal of Physical Anthropology*
757 **67**, 89-97.
- 758 Jungers, W. L. & Stern, J. T. 1981 Preliminary electromyographical analysis of brachiation in gibbon
759 and spider monkey. *International Journal of Primatology* **2**, 19-33.
- 760 Kilbourne, B. M. & Hoffman, L. C. 2013 Scale effects between body size and limb design in
761 quadrupedal mammals. *PloS one* **8**, e78392.
- 762 Kimura, T., Okada, M. & Ishida, H. 1979 Kinesiological characteristics of primate walking: its
763 significance in human walking. In *Environment, behavior, and morphology: Dynamic*
764 *interactions in primates* (ed. M. E. Morbeck, Preuschoft, H, Gomberg, N), pp. 297-311.
- 765 Lammers, A. R. & Gauntner, T. 2008 Mechanics of torque generation during quadrupedal arboreal
766 locomotion. *Journal of Biomechanics* **41**, 2388-2395.
- 767 Larney, E. & Larson, S. G. 2004 Compliant walking in primates: elbow and knee yield in primates
768 compared to other mammals. *American Journal of Physical Anthropology: The Official*
769 *Publication of the American Association of Physical Anthropologists* **125**, 42-50.
- 770 Larson, S. G. 2018 Nonhuman Primate Locomotion. *American Journal of Physical Anthropology* **165**,
771 705-725.
- 772 Larson, S. G., Schmitt, D., Lemelin, P. & Hamrick, M. 2001 Limb excursion during quadrupedal walking:
773 how do primates compare to other mammals? *Journal of Zoology* **255**, 353-365.
- 774 Larson, S. G. & Stern, J. T. 1987 EMG of chimpanzee shoulder muscles during knuckle-walking:
775 problems of terrestrial locomotion in a suspensory adapted primate. *Journal of Zoology* **212**,
776 629-655.
- 777 Larson, S. G. & Stern, J. T. 1989 The Role of Propulsive Muscles of the Shoulder During
778 Quadrupedalism in Vervet Monkeys (*Cercopithecus aethiops*). *Journal of Motor Behavior* **21**,
779 457-472.
- 780 Larson, S. G. & Stern, J. T. 2007 Humeral retractor EMG during quadrupedal walking in primates.
781 *Journal of Experimental Biology* **210**, 1204-1215.
- 782 Larson, S. G. & Stern, J. T. 2009 Hip extensor EMG and forelimb/hind limb weight support asymmetry
783 in primate quadrupeds. *American Journal of Physical Anthropology* **138**, 343-355.
- 784 Lawler, R. R. 2006 Sifaka positional behavior: Ontogenetic and quantitative genetic approaches.
785 *American Journal of Physical Anthropology* **131**, 261-271.
- 786 Maus, H.-M., Seyfarth, A. & Grimmer, S. 2011 Combining forces and kinematics for calculating
787 consistent centre of mass trajectories. *The Journal of Experimental Biology* **214**, 3511-3517.
- 788 McMahan, T. A., Valiant, G. & Frederick, E. C. 1987 Groucho running. *Journal of Applied Physiology* **62**,
789 2326-2337.
- 790 Miller, C. E., Johnson, L. E., Pinkard, H., Lemelin, P. & Schmitt, D. 2019 Limb phase flexibility in
791 walking: a test case in the squirrel monkey (*Saimiri sciureus*). *Frontiers in zoology* **16**, 1-13.
- 792 Muchlinski, M. N., Snodgrass, J. J. & Terranova, C. J. 2012 Muscle mass scaling in primates: an
793 energetic and ecological perspective. *American Journal of Primatology* **74**, 395-407.

- 794 Napier, J. R. 1967 Evolutionary aspects of primate locomotion. *American Journal of Physical*
795 *Anthropology* **27**, 333-341.
- 796 O'Neill, M. C. & Schmitt, D. 2012 The gaits of primates: center of mass mechanics in walking,
797 cantering and galloping ring-tailed lemurs, *Lemur catta*. *Journal of Experimental Biology* **215**,
798 1728-1739.
- 799 Ogihara, N., Makishima, H., Hirasaki, E. & Nakatsukasa, M. 2012 Inefficient use of inverted pendulum
800 mechanism during quadrupedal walking in the Japanese macaque. *Primates* **53**, 41-48.
- 801 Patel, B. A. 2009 Not so fast: Speed effects on forelimb kinematics in cercopithecine monkeys and
802 implications for digitigrade postures in primates. *American Journal of Physical Anthropology*
803 **140**, 92-112.
- 804 Patel, B. A., Larson, S. G. & Stern, J. T. 2012 Electromyography of wrist and finger flexor muscles in
805 olive baboons (*Papio anubis*). *Journal of Experimental Biology* **215**, 115-123.
- 806 Patel, B. A. & Polk, J. D. 2010 Distal forelimb kinematics in *Erythrocebus patas* and *Papio anubis*
807 during walking and galloping. *International Journal of Primatology* **31**, 191-207.
- 808 Patel, B. A., Wallace, I. J., Boyer, D. M., Granatosky, M. C., Larson, S. G. & Stern, J. T. 2015 Distinct
809 functional roles of primate grasping hands and feet during arboreal quadrupedal locomotion.
810 *Journal of Human Evolution* **88**, 79-84.
- 811 Pebsworth, P. A., Morgan, H. R. & Huffman, M. A. 2012 Evaluating home range techniques: use of
812 Global Positioning System (GPS) collar data from chacma baboons. *Primates* **53**, 345-355.
- 813 Pontzer, H., Raichlen, D. A. & Sockol, M. D. 2009 The metabolic cost of walking in humans,
814 chimpanzees, and early hominins. *Journal of Human Evolution* **56**, 43-54.
- 815 Pontzer, H. & Wrangham, R. W. 2004 Climbing and the daily energy cost of locomotion in wild
816 chimpanzees: implications for hominoid locomotor evolution. *Journal of Human Evolution* **46**,
817 315-333.
- 818 Prescott, M. J. & Buchanan-Smith, H. M. 2016 *Training Nonhuman Primates Using Positive*
819 *Reinforcement Techniques: A Special Issue of the journal of Applied Animal Welfare Science:*
820 *Psychology Press.*
- 821 Preuschoft, H. 2004 Mechanisms for the acquisition of habitual bipedality: are there biomechanical
822 reasons for the acquisition of upright bipedal posture? *Journal of Anatomy* **204**, 363-384.
- 823 Raichlen, D. A. 2004 Convergence of forelimb and hindlimb Natural Pendular Period in baboons
824 (*Papio cynocephalus*) and its implication for the evolution of primate quadrupedalism.
825 *Journal of Human Evolution* **46**, 719-738.
- 826 Rasmussen, S., Chan, A. & Goslow, G. 1978 The cat step cycle: electromyographic patterns for
827 hindlimb muscles during posture and unrestrained locomotion. *Journal of morphology* **155**,
828 253-269.
- 829 Reilly, S. M., McElroy, E. J. & Biknevicius, A. R. 2007 Posture, gait and the ecological relevance of
830 locomotor costs and energy-saving mechanisms in tetrapods. *Zoology* **110**, 271-289.
- 831 Reynolds, T. R. 1985 Mechanics of increased support of weight by the hindlimbs in primates.
832 *American Journal of Physical Anthropology* **67**, 335-349.
- 833 Rose, M. 1977 Positional behaviour of olive baboons (*Papio anubis*) and its relationship to
834 maintenance and social activities. *Primates* **18**, 59-116.
- 835 Schapiro, S. J., Bloomsmith, M. A. & Laule, G. E. 2003 Positive reinforcement training as a technique
836 to alter nonhuman primate behavior: quantitative assessments of effectiveness. *Journal of*
837 *Applied Animal Welfare Science* **6**, 175-187.
- 838 Schmitt, D. 1999 Compliant walking in primates. *Journal of Zoology* **248**, 149-160.
- 839 Schmitt, D. 2011 Translating Primate Locomotor Biomechanical Variables from the Laboratory to the
840 Field. In *Primate Locomotion* (ed. K. D'Août & E. E. Vereecke), pp. 7-27: Springer New York.
- 841 Schmitt, D., Cartmill, M., Griffin, T. M., Hanna, J. B. & Lemelin, P. 2006 Adaptive value of ambling gaits
842 in primates and other mammals. *Journal of Experimental Biology* **209**, 2042-2049.
- 843 Schmitt, D. & Hanna, J. B. 2004 Substrate alters forelimb to hindlimb peak force ratios in primates.
844 *Journal of Human Evolution* **46**, 237-252.

845 Schoonaert, K., D'Août, K., Samuel, D., Talloen, W., Nauwelaerts, S., Kivell, T. L. & Aerts, P. 2016 Gait
846 characteristics and spatio-temporal variables of climbing in bonobos (*Pan paniscus*).
847 *American Journal of Primatology*.

848 Shapiro, L. J., Anapol, F. C. & Jungers, W. L. 1997 Interlimb coordination, gait, and neural control of
849 quadrupedalism in chimpanzees. *American Journal of Physical Anthropology* **102**, 177-186.

850 Shapiro, L. J. & Jungers, W. L. 1994 Electromyography of back muscles during quadrupedal and
851 bipedal walking in primates. *American Journal of Physical Anthropology* **93**, 491-504.

852 St. George, L., Roy, S., Richards, J., Sinclair, J. & Hobbs, S. J. 2019 Surface EMG signal normalisation
853 and filtering improves sensitivity of equine gait analysis. *Comparative Exercise Physiology*, 1-
854 14.

855 Stern Jr, J. T. & Larson, S. G. 2001 Telemetered electromyography of the supinators and pronators of
856 the forearm in gibbons and chimpanzees: implications for the fundamental positional
857 adaptation of hominoids. *American Journal of Physical Anthropology: The Official Publication*
858 *of the American Association of Physical Anthropologists* **115**, 253-268.

859 Stern, J. T. & Susman, R. L. 1981 Electromyography of the gluteal muscles in *Hylobates*, *Pongo*, and
860 *pan*: Implications for the evolution of hominid bipedality. *American Journal of Physical*
861 *Anthropology* **55**, 153-166.

862 Swindler, D. R. & Wood, C. D. 1973 Atlas of primate gross anatomy.

863 Thorpe, S. K. S., Crompton, R. H. & Alexander, R. M. 2007 Orangutans use compliant branches to
864 lower the energetic cost of locomotion. *Biology letters* **3**, 253-256.

865 Toussaint, S., Llamasi, A., Morino, L. & Youlatos, D. 2020 The Central Role of Small Vertical Substrates
866 for the Origin of Grasping in Early Primates. *Current Biology*.

867 Vilensky, J. A. & Gankiewicz, E. 1990 Effects of growth and speed on hindlimb joint angular
868 displacement patterns in vervet monkeys (*Cercopithecus aethiops*). *American Journal of*
869 *Physical Anthropology* **81**, 441-449.

870 Vilensky, J. A. & Larson, S. G. 1989 Primate locomotion: utilization and control of symmetrical gaits.
871 *Annual Review of Anthropology* **18**, 17-35.

872 Young, J. W., Patel, B. A. & Stevens, N. J. 2007 Body mass distribution and gait mechanics in fat-tailed
873 dwarf lemurs (*Cheirogaleus medius*) and patas monkeys (*Erythrocebus patas*). *Journal of*
874 *Human Evolution* **53**, 26-40.

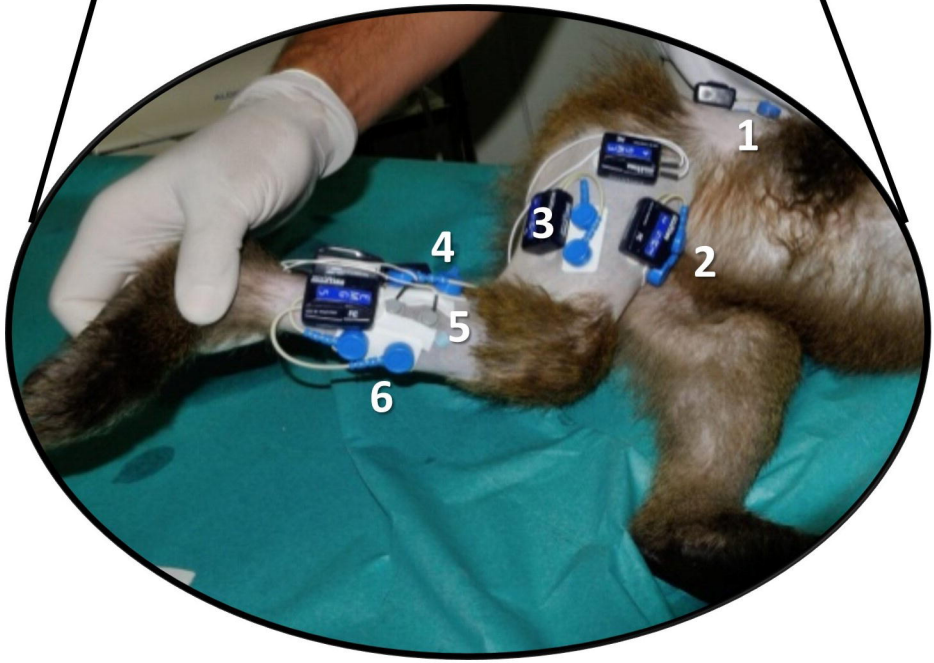
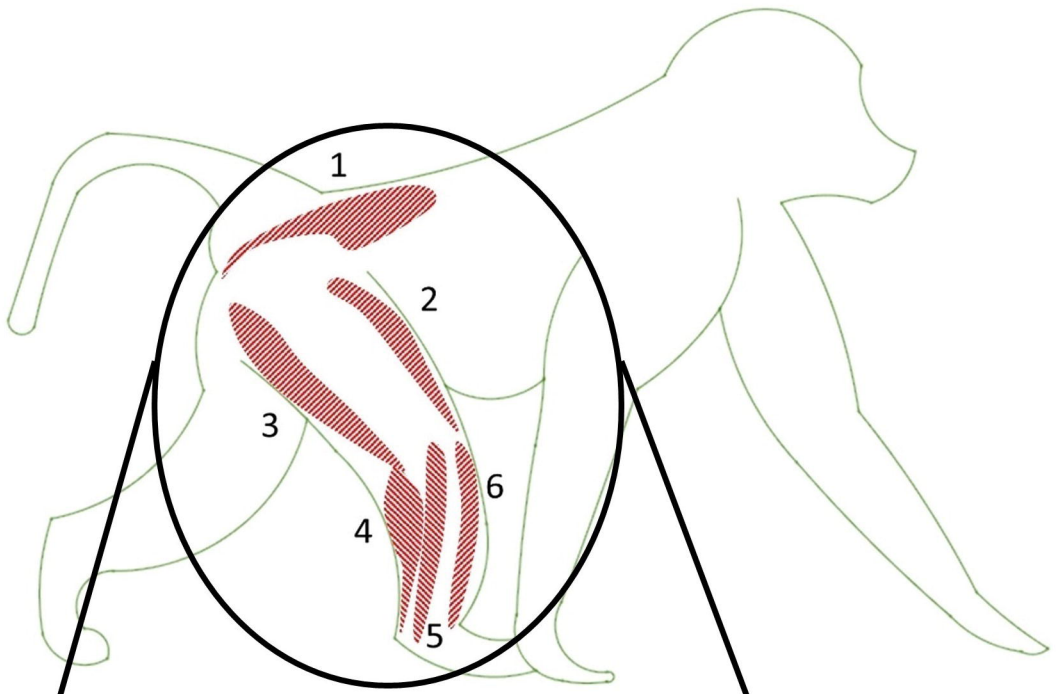
875 Young, J. W., Stricklen, B. M. & Chadwell, B. A. 2016 Effects of support diameter and compliance on
876 common marmoset (*Callithrix jacchus*) gait kinematics. *Journal of Experimental Biology* **219**,
877 2659-2672.

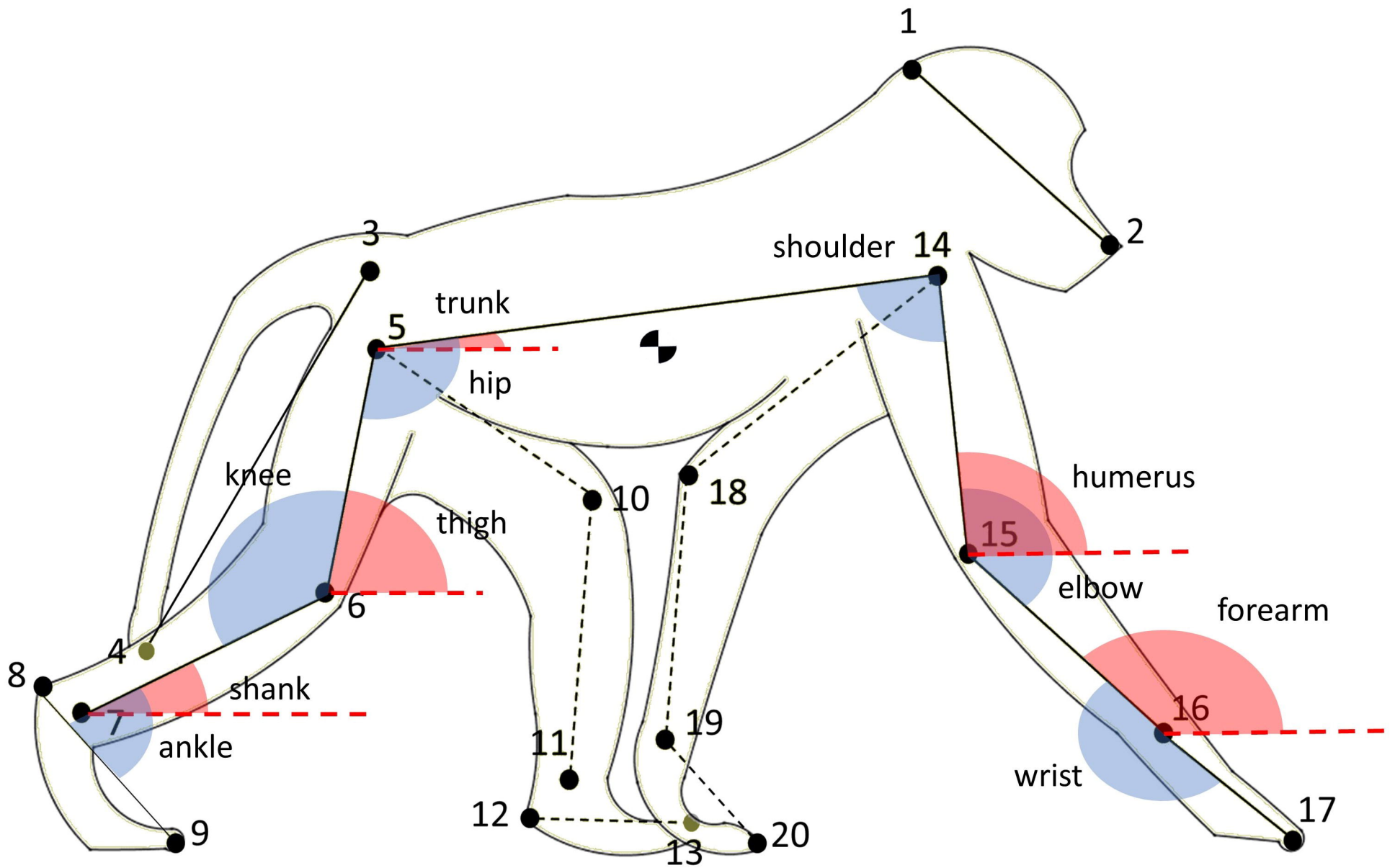
878 Zeininger, A., Shapiro, L. J. & Raichlen, D. A. 2017 Ontogenetic changes in limb postures and their
879 impact on effective limb length in baboons (*Papio cynocephalus*). *American Journal of*
880 *Physical Anthropology* **163**, 231-241.

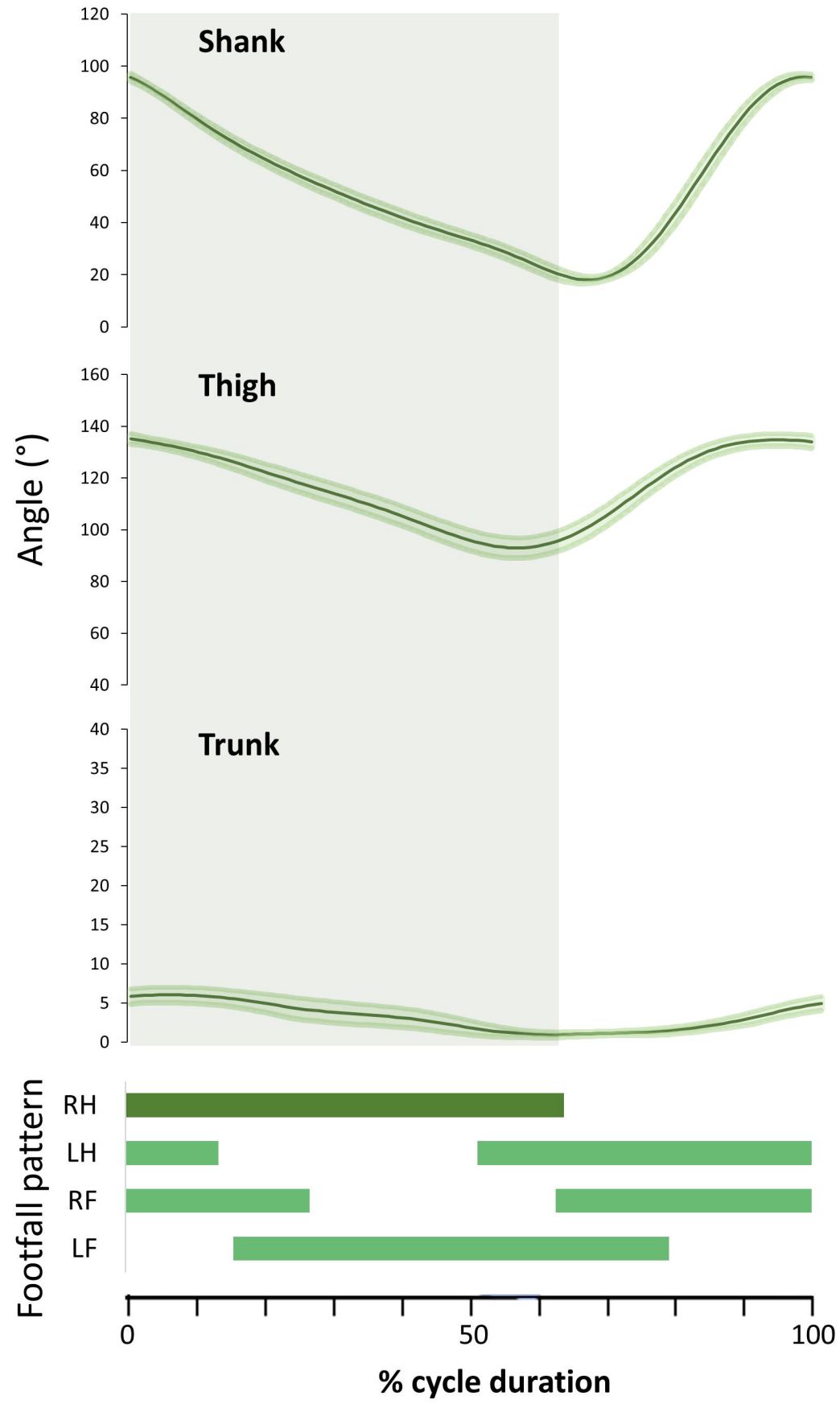
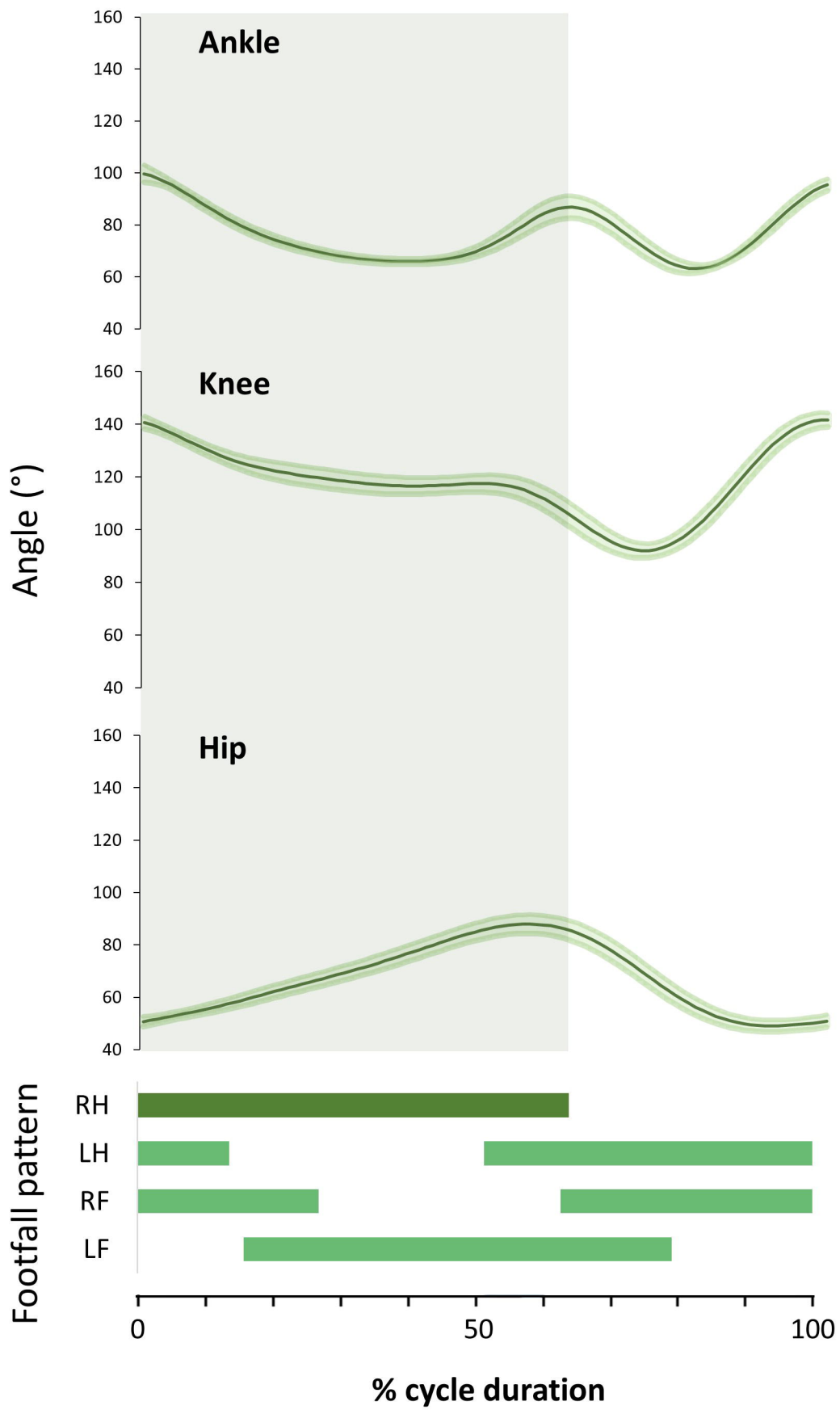
881 Zihlman, A. L. & Underwood, C. E. 2013 Locomotor anatomy and behavior of patas monkeys
882 (*Erythrocebus patas*) with comparison to vervet monkeys (*Cercopithecus aethiops*). *Anatomy*
883 *research international* **2013**.

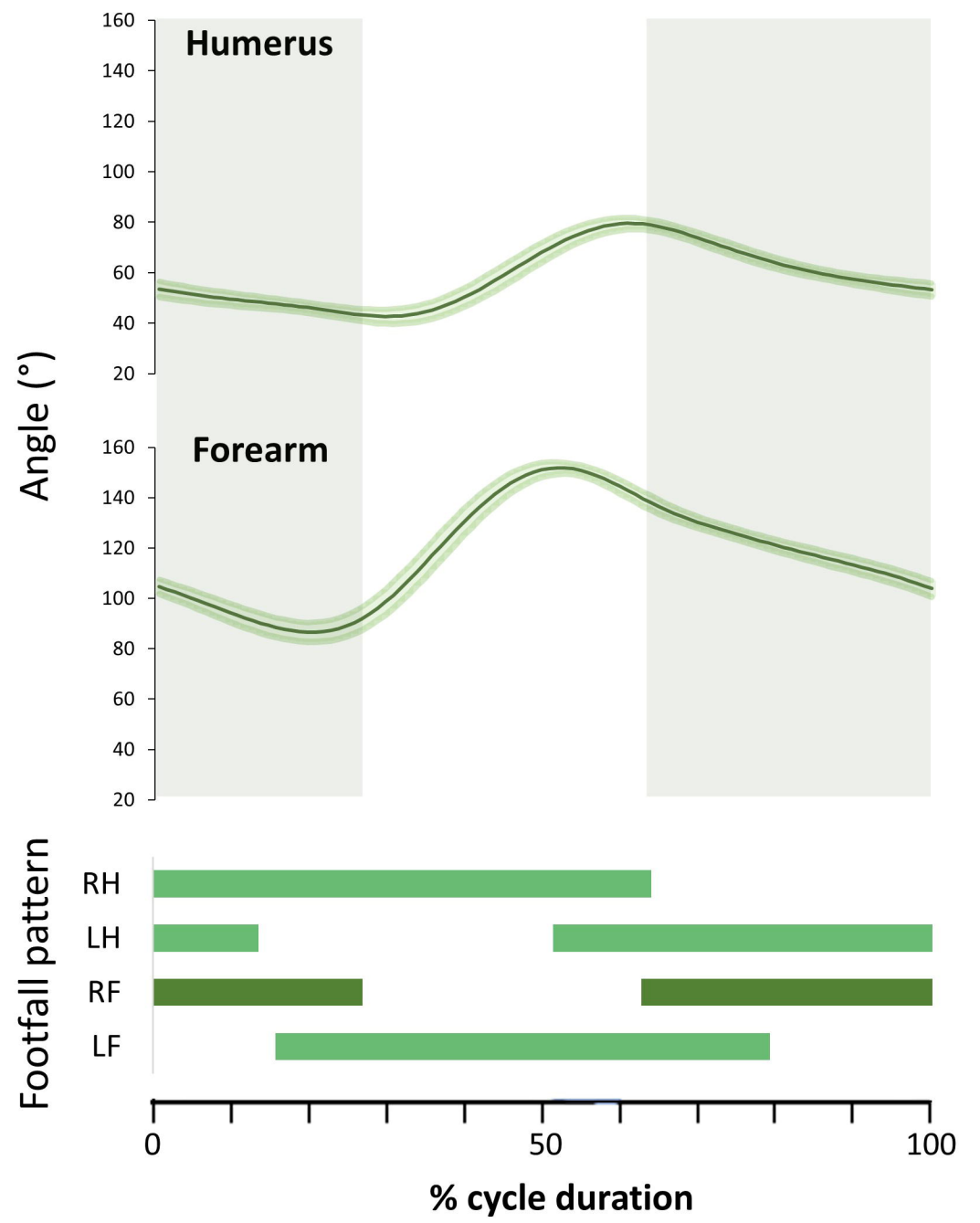
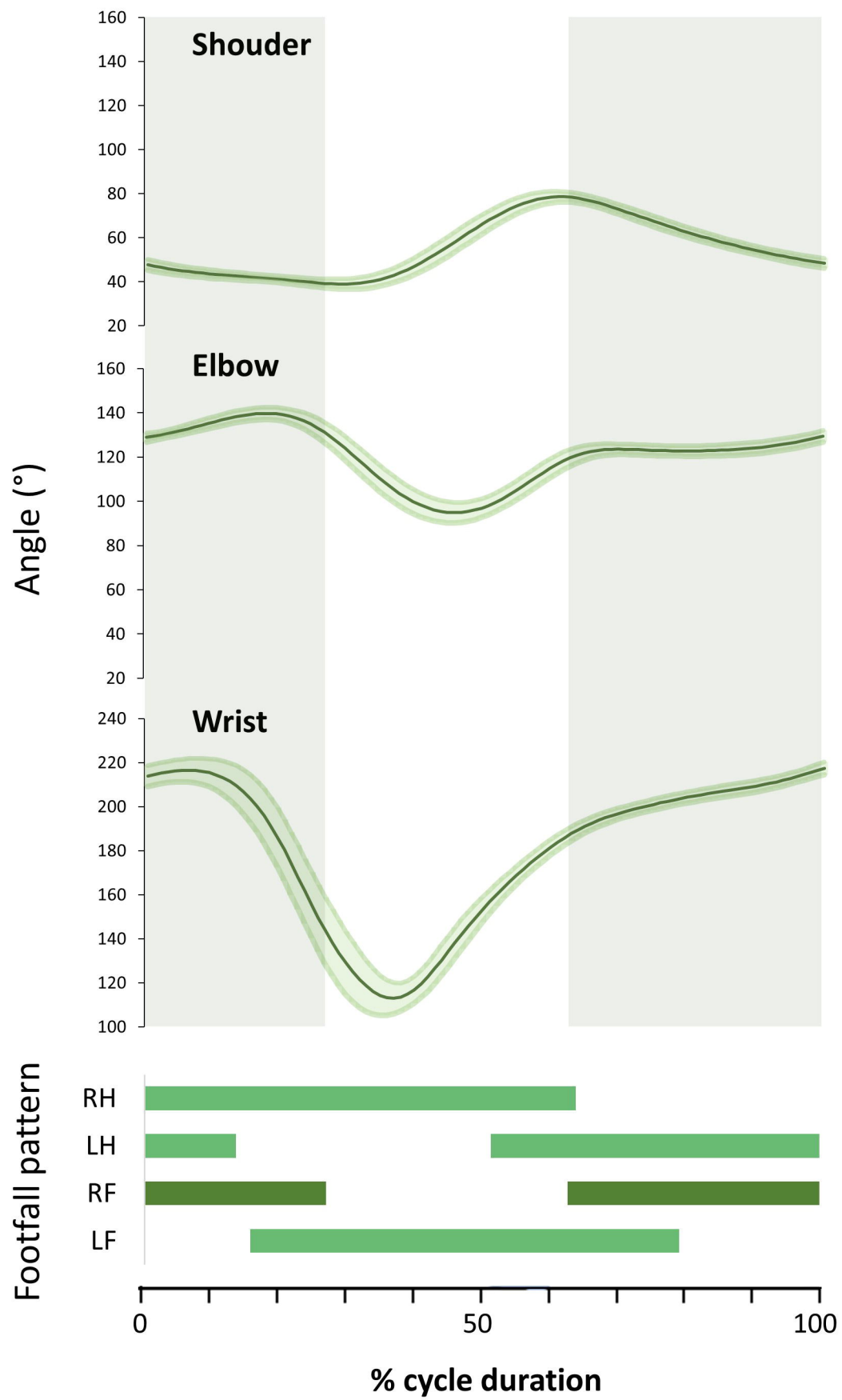
884 Zschorlich, V. 1989 Digital filtering of EMG-signals. *Electromyogr Clin Neurophysiol* **29**, 81-6.

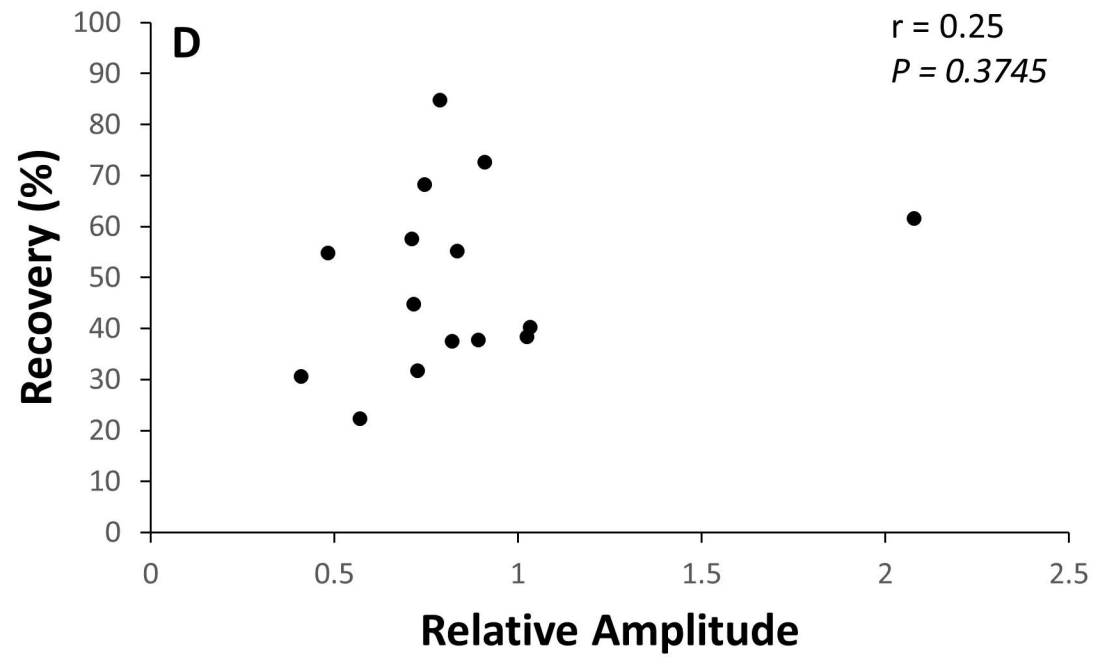
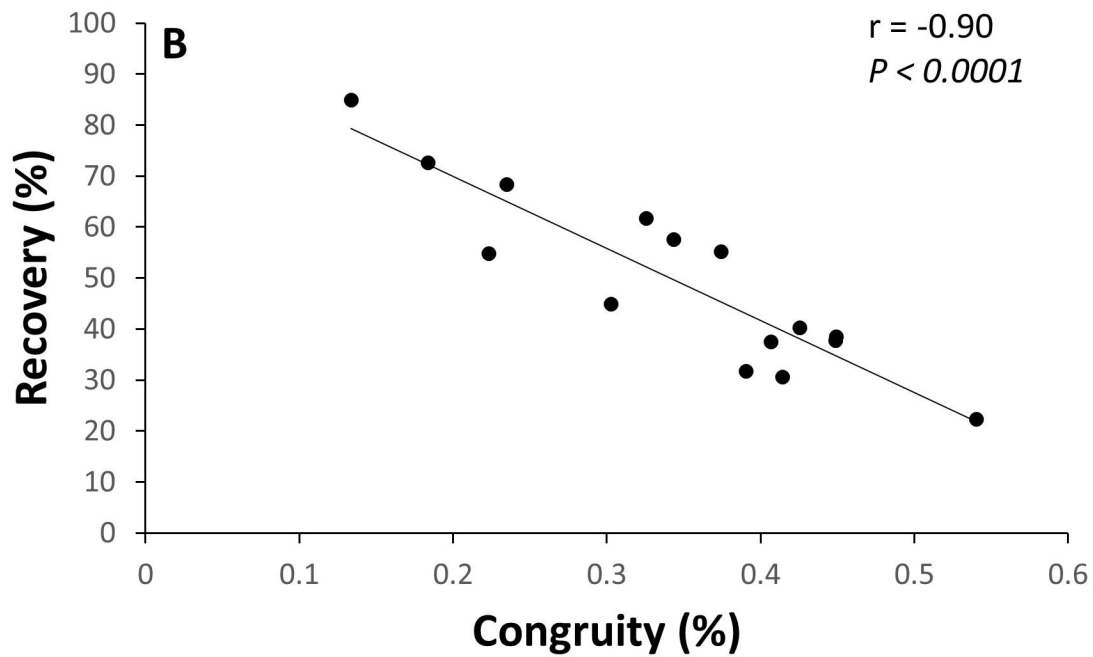
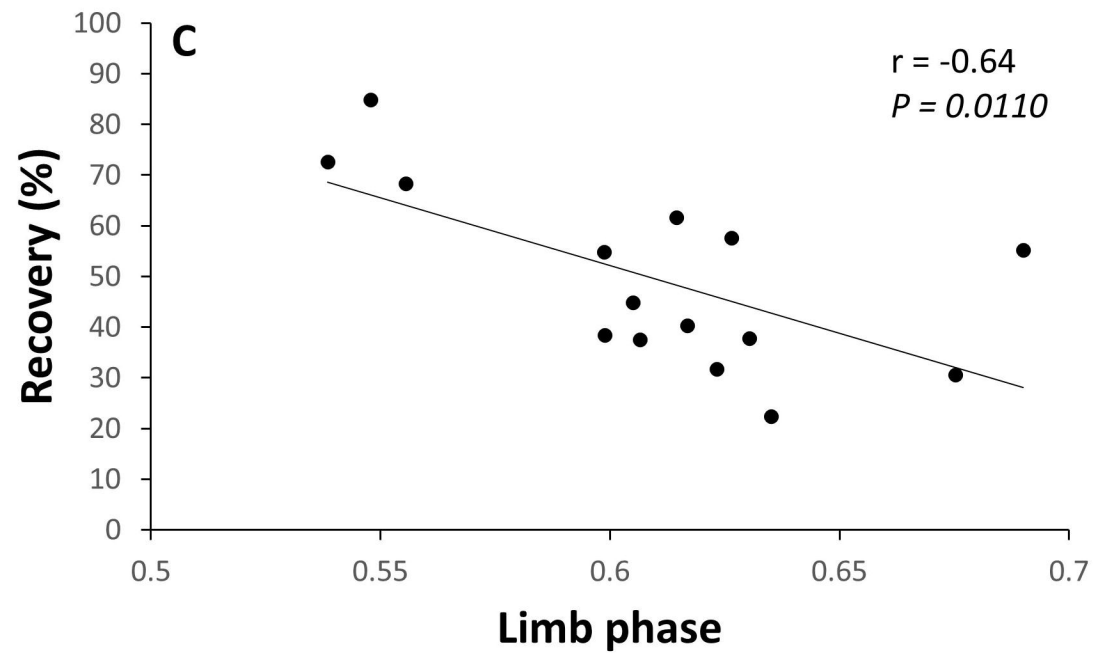
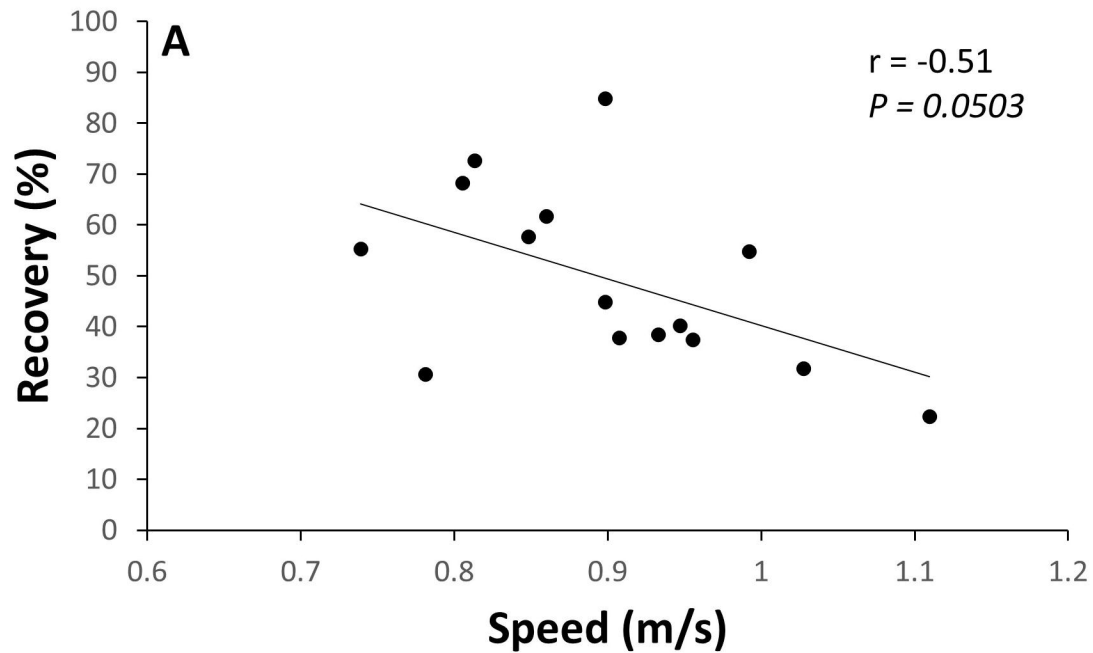
885

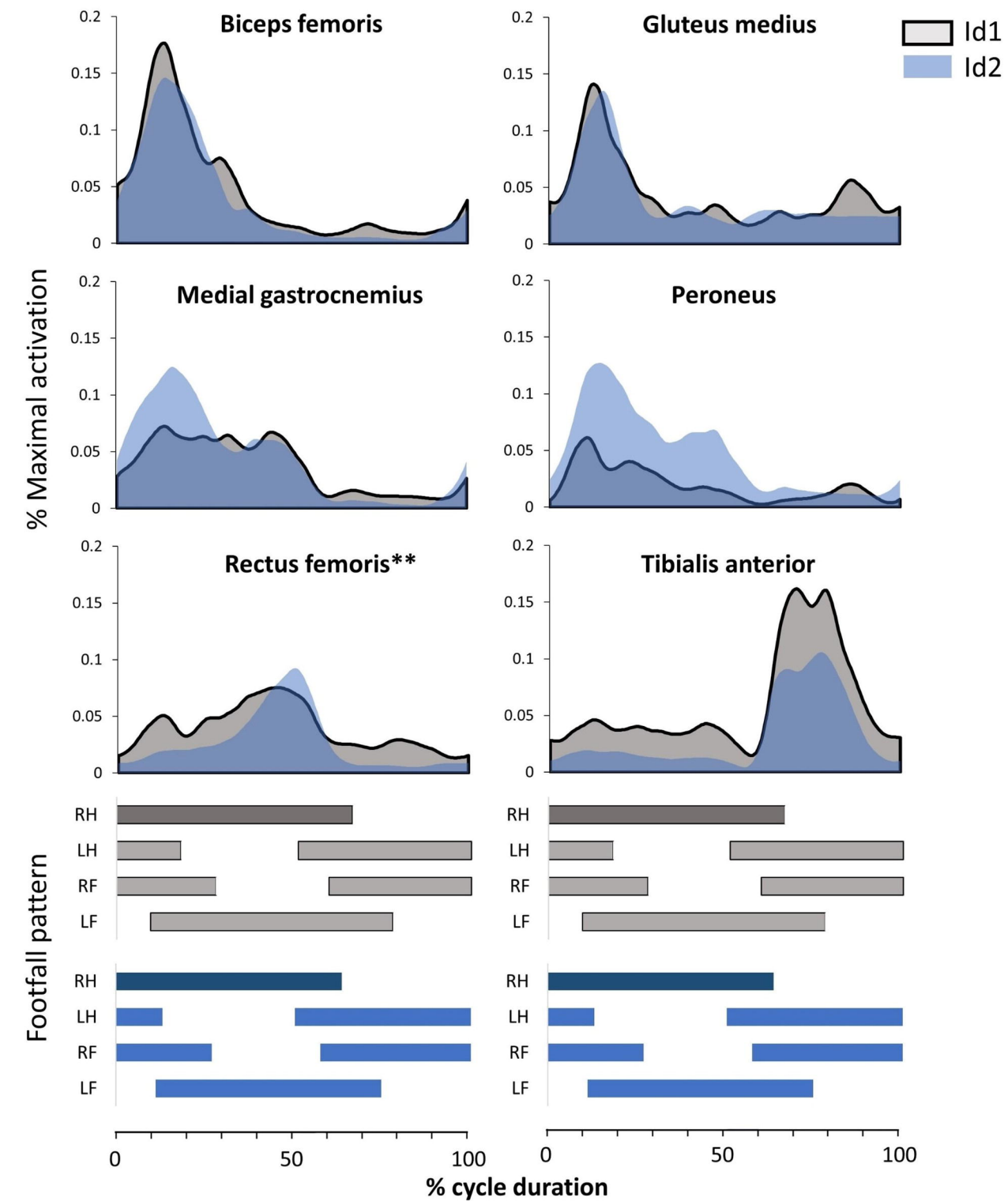










(A)**(B)**